Research Paper
Computational Methods for Differential Equations
http://cmde.tabrizu.ac.ir
Vol. *, No. *, *, pp. 1-26
DOI:10.22034/cmde.2026.70049.3462

Higher order multi-step methods for fractional differential equations

Mahmoud Ghasemzadeh[1], Ali Shokri[2,*], Mohammad Mehdizadeh Khalsaraei[1], and Mir Kamal Mirnia[3]
[1]Department of Mathematics, Faculty of Basic Science, University of Maragheh, Maragheh, Iran.
[2]Department of Applied Mathematics, Sahand University of Technology, Sahand New-Town, Tabriz, Iran.
[3]Department of Mathematics, Faculty of Mathematics, Statistics and Computer Science, University of Tabriz, Tabriz, Iran.

Abstract

This paper introduces **NewFLMM**, a novel family of high-order fractional linear multistep methods specifically designed to solve Caputo fractional differential equations. By integrating higher-order derivatives of the vector field, the proposed schemes significantly extend the stability regions beyond the inherent limits of classical fractional backward differentiation formulae (FBDF). We develop efficient recursive algorithms for coefficient generation and provide a rigorous stability analysis for orders $k = 2, 3$, and 4. The theoretical framework establishes both zero-stability and convergence properties. Numerical experiments on stiff and nonlinear systems confirm that NewFLMM provides superior accuracy and substantially broader stability domains than conventional methods. To facilitate implementation, comprehensive coefficient tables are provided.

Keywords. Fractional methods, Stability region, Numerical methods, Convergence order.
1991 Mathematics Subject Classification. 65L05, 65L20.

1. Introduction

To model dynamical systems the Fractional differential equations (FDEs) is pivotal framework since enable us to account memory effects [13, 14, 37] and also anomalous diffusion [5, 6, 15, 16, 18]. This model is important in sense encompassing the fields from viscoelasticity to advanced control systems [9, 22, 27, 30, 36, 42, 51].

The development of robust, high-order numerical algorithms remains a fundamental challenge not only for fractional differential equations but also for stochastic differential equations (SDEs) and financial models. In the context of SDEs, Ahmadian and Farkhondeh Rouz [2] conducted a stability analysis of the split-step θ-Milstein method for multi-dimensional problems, while Farkhondeh Rouz and Ahmadian [21] investigated the stability of improved backward Euler methods for neutral stochastic delay differential equations. Rathinasamy, Ahmadian, and Nair [40] further advanced the field by proposing second-order balanced stochastic Runge–Kutta methods with comprehensive multi-dimensional studies. Parallel to these stochastic advancements, efficient numerical techniques have also been developed for option pricing under various market conditions: Ahmadian, Ballestra, and Karimi [1] introduced an extremely efficient method for the Black–Scholes model with jumps, Ahmadian, Farkhondeh Rouz, and Ivaz [3] presented a robust algorithm for European options in illiquid markets, and Safdari-Vaighani, Ahmadian, and Javid-Jahromi [43] proposed an approximation scheme for option pricing under two-state continuous CAPM. Drawing inspiration from these stochastic and financial methodologies, where the balance between stability, accuracy, and computational efficiency is paramount. the present paper introduces the**NewFLMM** family for fractional differential equations. By incorporating higher-order derivative information into the multistep architecture, our proposed method significantly expands the stability region and reduces truncation errors, mirroring the stabilizing strategies that proved successful in the stochastic setting.

Alternatively, while the Fractional Linear Multistep Methods (FLMMs) introduced by Lubich [28, 29, 31] established a foundational framework, they require further refinement to address inherent limitations. Although the Fractional

Received: 04 November 2025; Accepted:28 July 2026.
* Corresponding author. Email: Ali_shokri@sut.ac.ir.

Table 1. Comparison of structural and stability properties.

Property	Standard FBDF	Classical FLMM	**Proposed NewFLMM**
Input Info.	$f(t, y)$	$f(t, y)$	f and f'
Stability ($k > 2$)	Restricted	Order-dependent	**Significantly Enlarged**
Stiff Handling	Poor	Moderate	**Excellent**
Global Error	Moderate	Moderate	**Minimal**

Backward Differentiation Formula (FBDF) has gained popularity due to its inheritance of classical BDF stability, its higher-order versions ($k > 2$) suffer from severely restricted stability regions, creating a significant bottleneck for stiff fractional systems [12, 25, 32, 49, 50]. To overcome these challenges, the present work introduces a structural refinement that leads to a remarkable expansion of the stability regions and a significant reduction in truncation errors compared to Lubich-type methods, as summarized in Table 1.

This paper is organized as follows: mathematical preliminaries is reviewed in section 2. Sections 3, 4, and 5 devote to the details of the systematic derivation of the NewFLMM family. provides rigorous convergence and stability analysis is discussed in section 6. Finally, numerical experiments on stiff and nonlinear problems to validating the theoretical findings are presented in section 7.

2. Preliminaries and mathematical foundations

The theoretical framework and computational tools required to be stablished is dealt in this section for developing and analysing of the proposed numerical scheme.

2.1. The Fractional Initial Value Problem (FIVP). The class of fractional initial value problems (FIVPs) is considered here which involves the Caputo fractional derivative of order $\beta \in (0, 1)$:

$$\begin{cases} {}_{t_0}^{C}D_t^{\beta} y(t) = f(t, y(t)), \quad t \in [t_0, T], \\ y(t_0) = y_0, \end{cases} \tag{2.1}$$

where $y : [t_0, T] \to \mathbb{R}^d$ and f is a nonlinear mapping. To ensure high-order convergence of the **NewFLMM**, we assume f and $y(t)$ are sufficiently smooth on $[t_0, T]$ [19, 38, 44, 48]. The singularities of the solutions obtained by NewFLMM at t_0, are exhibited through some numerical examples.

2.2. Caputo Fractional Derivative and Existence-Uniqueness Theory. Since the Caputo Fractional Derivative incorporates classical initial conditions, making FIVPs consistent with standard ODE theory [10, 11, 23, 34], then it is used mostly in engineering.

Definition 2.1. For a smooth function $y(t)$, the Caputo fractional derivative of order β is defined as:

$${}_{t_0}^{C}D_t^{\beta} y(t) = \frac{1}{\Gamma(1-\beta)} \int_{t_0}^{t} (t-s)^{-\beta} y'(s) ds, \quad 0 < \beta < 1. \tag{2.2}$$

Theorem 2.2 (Existence and Uniqueness)**.** *Consider the FIVP (2.1) on $\mathcal{D} = [t_0, T] \times [y_0 - \tau, y_0 + \tau]$. If $f(t, y)$ is continuous, bounded ($M = \sup|f|$), and satisfies the Lipschitz condition $|f(t, y) - f(t, z)| \le L|y - z|$, then there exists a unique solution $y(t) \in C[t_0, T^{]}$ where:*

$$T^* = \min\left\{T, t_0 + \left(\frac{\tau\Gamma(\beta+1)}{M}\right)^{1/\beta}\right\}. \tag{2.3}$$

Proof. The FIVP (2.1) is equivalent to the Volterra integral equation:

$$y(t) = y_0 + \frac{1}{\Gamma(\beta)} \int_{t_0}^{t} (t-s)^{\beta-1} f(s, y(s)) ds. \tag{2.4}$$

Define the operator $\mathcal{P}$ on $C[t_0, T^*]$ as $(\mathcal{P}y)(t) = y_0 + \frac{1}{\Gamma(\beta)} \int_{t_0}^{t} (t-s)^{\beta-1} f(s, y(s)) ds$. We first show $\mathcal{P}$ maps the ball $\mathcal{B} = \{y \in C[t_0, T^*] : \|y - y_0\|_\infty \leq \tau\}$ into itself. For any $y \in \mathcal{B}$:

$$\begin{aligned} |(\mathcal{P}y)(t) - y_0| &\leq \frac{1}{\Gamma(\beta)} \int_{t_0}^{t} (t-s)^{\beta-1} |f(s, y(s))| ds \\ &\leq \frac{M}{\Gamma(\beta)} \int_{t_0}^{t} (t-s)^{\beta-1} ds = \frac{M(t-t_0)^\beta}{\Gamma(\beta+1)}. \end{aligned} \tag{2.5}$$

By the definition of T^*, $\frac{M(T^*-t_0)^\beta}{\Gamma(\beta+1)} \leq \tau$, ensuring $\mathcal{P}y \in \mathcal{B}$. Next, we prove $\mathcal{P}$ is a contraction. For $y, z \in \mathcal{B}$:

$$|(\mathcal{P}y)(t) - (\mathcal{P}z)(t)| \leq \frac{L}{\Gamma(\beta)} \int_{t_0}^{t} (t-s)^{\beta-1} |y(s) - z(s)| ds. \tag{2.6}$$

By iterating $\mathcal{P}$ (Picard iteration) and applying the Banach Fixed Point Theorem [13, 19, 35, 36], it follows that $\mathcal{P}$ has a unique fixed point, which is the unique solution to (2.4). □

2.3. **Generating Functions and Miller's Algorithm.** The construction of Fractional Linear Multistep Methods (FLMMs) relies on the expansion of generating functions [33, 34, 41]. Let $\delta(z)$ be the characteristic polynomial of a classical k-step BDF method:

$$\delta(z) = \sum_{j=0}^{k} a_j z^j. \tag{2.7}$$

To discretize the fractional operator, we seek the coefficients of the fractional power of this generating function, $\omega(z) = (\delta(z))^\beta = \sum_{n=0}^{\infty} \omega_n z^n$. These coefficients, representing the convolution weights, are computed efficiently via Miller's algorithm [?]. Assuming $a_0 \neq 0$, the weights ω_n are obtained through the following recurrence:

$$\omega_0 = a_0^\beta, \quad \omega_n = \frac{1}{n a_0} \sum_{j=1}^{\min(n,k)} [j(\beta+1) - n]\, a_j \omega_{n-j}, \quad n \geq 1. \tag{2.8}$$

This recursive framework ensures both computational efficiency and numerical stability, forming the algorithmic foundation for the **NewFLMM** family.

3. Construction of NewFLMM: A second-derivative enhanced approach

In this section, we establish the theoretical foundation for the proposed **NewFLMM**. Here, β denotes the fractional order, while α_j and ω_j refer to the method's characteristic coefficients. Based on the work of Lubich [24], the discretization of the fractional integral in (2.1) is formulated via convolution quadrature:

$$\sum_{j=0}^{n} \alpha_j y_{n-j} = h^\beta \sum_{j=0}^{n} \omega_j f(t_{n-j}, y_{n-j}) + \mathcal{R}_n, \tag{3.1}$$

where $\mathcal{R}_n$ is the starting quadrature essential for maintaining the global order $\mathcal{O}(h^p)$ in the presence of initial singularities. The precision of this scheme is governed by the **Order Conditions**. For a convergence rate of order p, the linear difference operator $\Lambda_h[y(t); \beta]$ must satisfy:

$$\Lambda_h[y(t), t, \beta] = C_0 y(t_0) + \sum_{l=1}^{p-1} h^l C_l y^{(l)}(t_0) + \mathcal{O}(h^p). \tag{3.2}$$

The coefficients must satisfy the consistency relations:

$$C_0 = \sum_{j=0}^{k} \alpha_j = 0, \tag{3.3}$$

$$C_l = \frac{1}{l!}\sum_{j=0}^{k} j^l \alpha_j - \frac{1}{\Gamma(l+1-\beta)}\sum_{j=0}^{k} j^{l-\beta}\omega_j = 0, \quad l = 1, \dots, p-1. \tag{3.4}$$

3.1. **Fractional Backward Differentiation Formulae (FBDF).** The FBDF family [6, 30, 41] extends classical BDF schemes, known for their large stability regions in ODEs. The framework typically operates in two modes:

- **Implicit Mode:** $\sum_{j=0}^{n} \alpha_j y_{n-j} = h^\beta f(t_n, y_n)$.
- **Explicit Mode:** $\sum_{j=0}^{n} \alpha_j y_{n-j} = h^\beta f(t_{n-1}, y_{n-1})$.

3.2. **Generating Functions and Stability Constraints.** The β-th power of the k-th order backward difference operator yields the p-th order discretization. The design of FLMMs involves a critical trade-off between the region of absolute stability and the order of accuracy [34, 35, 45, 52]. Using Newton's backward difference interpolation, the generating function for a k-th order approximation is given by:

$$W_\beta(\zeta) = \left(\sum_{i=1}^{k} \frac{1}{i}(1-\zeta)^i\right)^\beta = \sum_{n=0}^{\infty} \omega_n \zeta^n. \tag{3.5}$$

While FBDFs are robust for $k \le 2$, they encounter severe limitations for $k > 2$, including restricted absolute stability regions and large principal error constants. These bottlenecks motivate the **NewFLMM** family, which incorporates higher-order information to expand the stability envelope. The core principle of this approach lies in the fact that a $(p+1)$-point backward difference provides a p-th order approximation of the first-order derivative. Consequently, the β-th power of the $(p+1)$-point backward difference approximation yields a p-th order discretization of the β-th derivative [36, 40] . The corresponding weights $\{\omega_n\}$ are obtained as the coefficients of the Taylor series expansion of the generating functions.

(1) **Restricted stability regions:** The absolute stability domain shrinks significantly, making the scheme unsuitable for *stiff* fractional systems.
(2) **Large principal error constants:** Although the theoretical order is high, the absolute magnitude of the truncation error remains substantial.

These computational bottlenecks provide the primary motivation for the **NewFLMM** family. By strategically incorporating higher-order information into the multistep structure, the proposed method effectively expands the stability envelope and minimizes the error constants, thereby facilitating efficient long-term integration of complex fractional dynamics [7, 20, 44, 47].

3.3. **Derivation of the Generating Function.** The core of designing high-order FLMMs lies in the construction of appropriate generating functions. The following theorem, which we establish based on Newton's interpolation, provides the analytical form for these functions.

Theorem 3.1. *[Generating Function Construction] The generating function $G^k_\beta(\xi)$ for a k-th order fractional multistep approximation, derived from the k-th order backward difference operator, is given by:*

$$G^k_\beta(\xi) = \left(\sum_{i=1}^{k} \frac{1}{i}\left[1 + (-1)^i \binom{k}{i}\xi^i\right]\right)^\beta. \tag{3.6}$$

Proof. Consider the function $f(\xi)$ and its interpolating polynomial $P(\xi)$ of degree k. Based on Newton's backward difference interpolation formula [22, 36], the function at any point $\xi = \xi_i + \theta h$ is approximated as:

$$f(\xi) \simeq P(\xi) = f_i + \theta\nabla f_i + \frac{\theta(\theta+1)}{2!}\nabla^2 f_i + \cdots + \frac{\theta(\theta+1)\dots(\theta+k-1)}{k!}\nabla^k f_i, \tag{3.7}$$

where ∇ denotes the backward difference operator, $\nabla f_i = f_i - f_{i-1}$. To find the derivative approximation at $\xi = \xi_i$ (corresponding to $\theta = 0$), we have:

$$f'(\xi_i) \simeq \frac{1}{h}\frac{dP}{d\theta}\bigg|_{\theta=0} = \frac{1}{h}\left(\nabla f_i + \frac{1}{2}\nabla^2 f_i + \cdots + \frac{1}{k}\nabla^k f_i\right). \tag{3.8}$$

In terms of the generating function, the shift operator is identified with ξ, such that $\nabla = 1 - \xi$. By taking the β-th power to extend this to fractional orders, we consider the following cases:

Case $k = 1$**::** $G^1_\beta(\xi) = (1-\xi)^\beta$.

Case $k = 2$**::** $f'(\xi_i) \simeq \frac{1}{h}(\nabla + \frac{1}{2}\nabla^2)f_i = \frac{1}{h}(\frac{3}{2} - 2\xi + \frac{1}{2}\xi^2)f_i$, which leads to $G^2_\beta(\xi) = (\frac{3}{2} - 2\xi + \frac{1}{2}\xi^2)^\beta$.

Generalizing this inductive process for an arbitrary step-number k yields the desired general relation. □

3.4. **Numerical Stability and Motivation for NewFLMM.** A primary challenge in the practical implementation of FLMMs is designing schemes that maintain a large region of absolute stability without sacrificing high-order accuracy [23, 33]. While standard FBDFs leverage the generating functions derived in Theorem 3.1 to ensure zero-stability, they often suffer from **restricted stability regions and large principal error constants** as the step-number k increases, making them ill-suited for long-term integration.

Furthermore, the computational overhead associated with the non-local nature of fractional weights grows significantly over time. These limitations motivate the development of the **NewFLMM** family. By strategically incorporating higher-order derivatives of the vector field into the multistep framework, the proposed method enhances the stability-to-error ratio and relaxes the constraints on the coefficients. Specifically, the **NewFLMM** is designed to ensure that for orders $k = 3$ and $k = 4$, the $A(\alpha)$-stability angle remains significantly wider than that of conventional FBDF—a prerequisite for handling stiff fractional problems.

While existing literature on second-derivative multistep methods for classical ODEs (e.g., the seminal work of Enright [23, 38]) demonstrates their superiority in stability, their extension to fractional-order equations remains largely unexplored. The **NewFLMM** fills this critical gap by marrying the concept of second-derivative inclusion with the convolution quadrature framework, effectively bypassing the Dahlquist-like barriers inherent in standard fractional formulas.

4. Construction and theoretical framework of the NewFLMM methodology

To address the inherent limitations of traditional Fractional Linear Multistep Methods (FLMMs), we propose the **NewFLMM** framework. Unlike conventional methods that rely solely on the evaluation of the vector field $f(t, y(t))$, the proposed approach incorporates higher-order analytical information by utilizing total derivatives of the vector field, $f^{(m)}(t, y(t))$. This strategic augmentation effectively circumvents the stability-accuracy trade-offs and significantly enhances the stability-to-error ratio.

The general structure of the k-step **NewFLMM** for the fractional order β is formulated as follows:

$$\sum_{j=0}^{k} \alpha_j y_{n-j} = h^\beta \sum_{j=0}^{k} \omega_j f_{n-j} + h^{\beta+1} \sum_{j=0}^{k} \gamma_j g_{n-j}, \tag{4.1}$$

where $g(t, y) = f'(t, y)$. While the theoretical order is dictated by the consistency conditions, the practical selection of coefficients α_j and γ_j is primarily guided by the **Schur-Cohn criterion** [7, 8, 31]. This ensures that the method remains zero-stable, a critical requirement for maintaining robustness in orders $p \geq 3$, where traditional FBDF schemes typically exhibit instability.

4.1. **The Proposed Numerical Scheme.** While analytical differentiation of the vector field may appear demanding, it remains highly feasible and computationally efficient for a broad class of dynamical systems, especially when restricted to the first few total derivatives. We define the **NewFLMM** for solving the fractional differential equation (2.1) via the following multistep framework:

$$\sum_{j=0}^{n} \alpha_j y_{n-j} = h^\beta \sum_{j=0}^{n} \omega_j f_{n-j} + \sum_{m=1}^{M} h^{\beta+m} \sum_{j=0}^{n} \eta_{j,m} f^{(m)}_{n-j}, \tag{4.2}$$

where $h > 0$ denotes the uniform step size, and $\{\alpha_j, \omega_j, \eta_{j,m}\}$ are the characteristic real coefficients of the method. The integer M signifies the highest order of the total derivative incorporated into the scheme.

The strategic inclusion of the terms $\eta_{j,m}$ introduces additional **degrees of freedom** into the quadrature weights. This flexibility is the cornerstone of the NewFLMM, as it allows for the simultaneous optimization of the stability domain and the reduction of principal error constants, all while maintaining the desired algebraic order of accuracy. For the practical purposes of this study, we focus on the case $M = 1$ (second-derivative inclusion), which provides an optimal balance between computational complexity and stability enhancement.

4.2. **Order Conditions and Truncation Error Analysis.** The precision of the proposed scheme is governed by the linear difference operator $\Lambda_h[y(t); \beta]$. For the method to achieve an algebraic convergence rate of order p, this operator must vanish for all polynomials of degree $q < p$. The operator is defined as:

$$\Lambda_h[y(t), h, \beta] = \sum_{j=0}^{n} \alpha_j y(t_{n-j}) - h^{\beta} \sum_{j=0}^{n} \omega_j D^{\beta} y(t_{n-j}) - \sum_{m=1}^{M} h^{\beta+m} \sum_{j=0}^{n} \eta_{j,m} D^{\beta+m} y(t_{n-j}). \tag{4.3}$$

By applying Taylor's expansion of $y(t_{n-j})$ around t_n and utilizing the fractional derivative property $D^{\alpha}(t - t_0)^k = \frac{\Gamma(k+1)}{\Gamma(k+1-\alpha)}(t - t_0)^{k-\alpha}$ into the linear operator, we obtain:

$$\begin{aligned} \Lambda_h[y(t), h, \beta] &= \sum_{j=0}^{n} \alpha_j \left(\sum_{k=0}^{\infty} \frac{(-j)^k}{k!} h^k y_n^{(k)} \right) \\ &\quad - h^{\beta} \sum_{j=0}^{n} \omega_j \left(\sum_{k=0}^{\infty} \frac{(-j)^{k-\beta}}{\Gamma(k+1-\beta)} h^k y_n^{(k)} \right) \\ &\quad - \sum_{m=1}^{M} h^{\beta+m} \sum_{j=0}^{n} \eta_{j,m} \left(\sum_{k=0}^{\infty} \frac{(-j)^{k-\beta-m}}{\Gamma(k+1-\beta-m)} h^k y_n^{(k)} \right). \end{aligned} \tag{4.4}$$

By equating the coefficients of $h^l y_n^{(l)}$ to zero, we derive the **Generalized Order Conditions** for the NewFLMM:

$$C_0 = \sum_{j=0}^{n} \alpha_j = 0, \tag{4.5}$$

$$C_l = \frac{1}{l!} \sum_{j=0}^{n} (-j)^l \alpha_j - \frac{1}{\Gamma(l+1-\beta)} \sum_{j=0}^{n} (-j)^{l-\beta} \omega_j - \sum_{m=1}^{M} \frac{\sum_{j=0}^{n} (-j)^{l-\beta-m} \eta_{j,m}}{\Gamma(l+1-\beta-m)} = 0, \tag{4.6}$$

for $l = 1, 2, \ldots, p - 1$.

Remark 4.1 (Degrees of Freedom and Stability Constraints)**.** An analysis of the available degrees of freedom suggests that a high algebraic order is theoretically attainable for implicit formulations. However, the selection of coefficients $\{\alpha_j\}$ is strictly constrained by the **Schur-Cohn criterion** to ensure zero-stability. This requirement often imposes a practical upper bound on the achievable order p, particularly for multi-step configurations where the root condition must be satisfied to prevent numerical divergence.

5. The proposed NewFLMM algorithmic framework

In this section, we delineate a systematic procedure for the construction of a p-th order **NewFLMM**. The methodology integrates the spectral properties of fractional generating functions with the additional degrees of freedom provided by higher-order derivatives to optimize the stability-accuracy trade-off [4, 8, 17].

5.1. **General construction procedure.** The synthesis of the NewFLMM of order p proceeds through a three-stage recursive pipeline:

Stage 1: Spectral kernel construction. The foundation of the scheme is the fractional generating function $G_\beta^p(\xi)$, which encapsulates the non-local history of the fractional operator. Based on the p-th order BDF family, it is defined as:

$$G_\beta^p(\xi) = \left(\sum_{i=1}^{p} \frac{1}{i}(1-\xi)^i\right)^\beta = \sum_{j=0}^{\infty} \omega_j \xi^j. \tag{5.1}$$

Stage 2: Recursive synthesis of coefficients α_j. The coefficients α_j (the left-hand side weights) are extracted via *Miller's recursive algorithm* to ensure numerical stability. The coefficients for $j < p$ are initialized using the power-series expansion, while for $j \geq p$, they follow a p-th order linear recurrence. The boundary coefficients $\{\alpha_n, \alpha_{n-1}, \dots, \alpha_{n-p+1}\}$ are subsequently adjusted by enforcing the consistency conditions $C_l = 0$.
Stage 3: Computation of optimized auxiliary weights. To ensure global consistency and account for the second-derivative enhancement, the weight vector γ (or $\eta_{j,m}$ for derivatives) is synthesized. By enforcing the generalized order conditions derived in the previous section, the primary auxiliary weight is calculated as:

$$\gamma = \Gamma(p-\beta+1)n^{\beta-p+1}\left[\frac{1}{(p-1)!}\sum_{q=0}^{n}(n-q)^{p-1}\alpha_q - \frac{n^{p-\beta-2}}{\Gamma(p-\beta-1)}\right]. \tag{5.2}$$

This recursive refinement ensures that the starting quadrature $\mathcal{R}_n$ remains sub-dominant to the total discretization error.

5.2. **Numerical realization for specific orders.** To facilitate the practical implementation of the **NewFLMM**, we provide the explicit recursive structures for standard orders of accuracy $p = 2, 3$, and 4.

Case $p = 2$ (Quadratic Precision):: The generating function is $G_\beta^2(\xi) = (\frac{3}{2} - 2\xi + \frac{1}{2}\xi^2)^\beta$. The multistep coefficients α_j are computed via the following three-term recurrence for $j = 2, \dots, n-2$:

$$\alpha_j = \frac{4}{3}\left(1 - \frac{\beta+1}{j}\right)\alpha_{j-1} + \frac{1}{3}\left(\frac{2(\beta+1)}{j} - 1\right)\alpha_{j-2}. \tag{5.3}$$

The boundary weights $\{\alpha_n, \alpha_{n-1}\}$ are determined by satisfying the consistency conditions $C_0 = C_1 = 0$, and the auxiliary weight γ is given by:

$$\gamma = \Gamma(2-\beta)n^\beta\left(\sum_{p=0}^{n}(n-p)\alpha_p - \frac{n^{-\beta}}{\Gamma(-\beta)}\right). \tag{5.4}$$

Case $p = 3$ (Cubic Precision):: The generating function is $G_\beta^3(\xi) = (\frac{11}{6} - 3\xi + \frac{3}{2}\xi^2 - \frac{1}{3}\xi^3)^\beta$. The coefficients satisfy the four-term recurrence for $j = 3, \dots, n-3$:

$$\alpha_j = \frac{18}{11}\left(1 - \frac{\beta+1}{j}\right)\alpha_{j-1} + \frac{9}{11}\left(\frac{2(\beta+1)}{j} - 1\right)\alpha_{j-2} + \frac{2}{11}\left(1 - \frac{3(\beta+1)}{j}\right)\alpha_{j-3}. \tag{5.5}$$

The boundary coefficients are determined by $C_0 = C_1 = C_2 = 0$, with γ evaluated as:

$$\gamma = \Gamma(3-\beta)n^{\beta-2}\left(\frac{1}{2}\sum_{p=0}^{n}(n-p)^2\alpha_p - \frac{n^{1-\beta}}{\Gamma(2-\beta)}\right). \tag{5.6}$$

Case $p = 4$ (Quartic Precision):: The generating function is $G_\beta^4(\xi) = (\frac{25}{12} - 4\xi + 3\xi^2 - \frac{4}{3}\xi^3 + \frac{1}{4}\xi^4)^\beta$. The coefficients follow the five-term recurrence for $j = 4, \dots, n-4$:

$$\begin{aligned}\alpha_j =& \frac{48}{25}\left(1 - \frac{\beta+1}{j}\right)\alpha_{j-1} + \frac{36}{25}\left(\frac{2(\beta+1)}{j} - 1\right)\alpha_{j-2} \\ &+ \frac{16}{25}\left(1 - \frac{3(\beta+1)}{j}\right)\alpha_{j-3} + \frac{3}{25}\left(\frac{4(\beta+1)}{j} - 1\right)\alpha_{j-4}.\end{aligned} \tag{5.7}$$

The weights $\{\alpha_n, \dots, \alpha_{n-3}\}$ are evaluated via the system $C_l = 0$ for $l = 0, \dots, 3$, and γ follows:

$$\gamma = \Gamma(4-\beta) n^{\beta-3} \left(\frac{1}{6} \sum_{p=0}^{n} (n-p)^3 \alpha_p - \frac{n^{2-\beta}}{\Gamma(3-\beta)} \right). \tag{5.8}$$

5.3. **Algorithm summary.** The practical implementation of the **NewFLMM** is summarized in the following systematic steps:

(1) **Kernel Initialization:** Select the target algebraic order p and construct the corresponding BDF-based generating function $G_\beta^p(\xi)$ as the spectral foundation.
(2) **Weight Generation:** Compute the internal multistep weights α_j using the p-th order *Miller recurrence* relations derived in the previous section.
(3) **Boundary & Consistency Tuning:** Solve the $(p+1) \times (p+1)$ linear system $C_l = 0$ (for $l = 0, \dots, p$) to determine the boundary coefficients $\{\alpha_n, \dots, \alpha_{n-p+1}\}$ and the auxiliary weight γ. This step ensures the elimination of the starting quadrature error.
(4) **Derivative Evaluation & Evolution:** Incorporate the total derivative f'_n. While f' can be evaluated analytically for many dynamical systems, it can also be approximated using a p-th order **Backward Difference Formula (BDF)** to maintain the global convergence rate and preserve the causality of the scheme.
(5) **System Update:** Evolve the discrete solution y_n by solving the resulting (often implicit) algebraic system at each time step.

To maintain the flow of the theoretical discussion, the tabulated coefficients for various values of β and p are provided in the Appendix.

6. Stability and convergence analysis of the NewFLMM framework

In this section, we investigate the numerical stability and global error propagation of the proposed **NewFLMM**. The analysis is performed using the linear fractional test equation:

$$ {}_{t_0}^{C}D_t^{\beta} y(t) = \lambda y(t), \quad 0 < \beta < 1, \quad \lambda \in \mathbb{C}, \tag{6.1}$$

with the initial condition $y(t_0) = y_0$, whose analytical solution is $y(t) = y_0 E_\beta(\lambda (t-t_0)^\beta)$.

Theorem 6.1. *(Global Error Representation and Convergence) Let $\tilde{e}_n = y(t_n) - y_n$ be the global discretization error at step n. Under the assumption of p-th order consistency, the error propagation for the NewFLMM is governed by:*

$$\tilde{e}_n = \sum_{s=1}^{k} d_s \xi_s^n - \frac{Q}{h^\beta \lambda \left(\sum_{j=0}^{k} \omega_j + \sum_{m=1}^{M} h^m \frac{\lambda_m}{\lambda} \eta_{j,m} \right)}, \tag{6.2}$$

where d_s are constants determined by initial perturbations, Q represents the aggregate local truncation error of order $\mathcal{O}(h^{p+\beta})$, and ξ_s are the roots of the ***generalized characteristic polynomial****:*

$$\Pi(\xi; z) = \sum_{j=0}^{k} \left(\alpha_j - z\omega_j - \sum_{m=1}^{M} z h^m \frac{\lambda_m}{\lambda} \eta_{j,m} \right) \xi^{k-j} = 0, \tag{6.3}$$

where $z = \lambda h^\beta$. The scheme is convergent with order p if it is zero-stable.

Proof. Let $y(t_n)$ and y_n be the exact and numerical solutions, respectively. The exact solution satisfies the perturbed relation:

$$\sum_{j=0}^{k} \alpha_j y(t_{n-j}) = h^\beta \sum_{j=0}^{k} \omega_j f(t_{n-j}, y(t_{n-j})) + \sum_{m=1}^{M} h^{\beta+m} \sum_{j=0}^{k} \eta_{j,m} f^{(m)}(t_{n-j}, y(t_{n-j})) + T_n, \tag{6.4}$$

where $T_n = \mathcal{O}(h^{p+\beta})$. Defining the global error $\tilde{e}_n = y(t_n) - y_n$ and linearizing the vector fields f and $f^{(m)}$ around the exact trajectory (with $\lambda_0 = \frac{\partial f}{\partial y}$ and $\lambda_m = \frac{\partial f^{(m)}}{\partial y}$), we obtain the following linear difference equation:

$$\sum_{j=0}^{k} \left(\alpha_j - h^{\beta}\lambda_0\omega_j - \sum_{m=1}^{M} h^{\beta+m}\lambda_m\eta_{j,m} \right) \tilde{e}_{n-j} = T_n - R_n, \tag{6.5}$$

where R_n denotes the round-off error. By solving the associated homogeneous part, the error is expressed as a linear combination of the roots ξ_s of the characteristic equation (6.3). For zero-stability, it is mandatory that $|\xi_s| \le 1$, and any root with $|\xi_s| = 1$ must be simple. Under these conditions, the non-homogeneous part (the particular solution) is dominated by Q/h^{β}, which, given $T_n = \mathcal{O}(h^{p+\beta})$, confirms the global convergence rate of $\mathcal{O}(h^p)$. □

6.1. **Implicit Formulation and Stability Domain Derivation.** The implicit NewFLMM-I is engineered to achieve high-order algebraic precision by incorporating the first-order total derivative of the vector field. The fundamental discrete relation for the implicit configuration is formulated as:

$$\sum_{j=0}^{n} \alpha_j y_{n-j} = h^{\beta}\left(\gamma f(t_n, y_n) + h f'(t_n, y_n)\right). \tag{6.6}$$

To facilitate a derivative-free implementation while preserving the stability benefits of the second-derivative term, we employ a p-th order backward finite difference approximation for f'_n. For the quadratic case, utilizing $f'_n \approx (f_n - f_{n-2})/(2h)$ and substituting it into (6.6) yields the following **Refined Implicit Recurrence**:

$$\sum_{j=0}^{n} \alpha_j y_{n-j} = h^{\beta}\left[\left(\gamma + \frac{1}{2}\right) f_n - \frac{1}{2} f_{n-2}\right]. \tag{6.7}$$

To investigate the absolute stability, we apply the test equation $f(t, y) = \lambda y$. Let $\bar{z} = \lambda h^{\beta}$ denote the stability parameter. The stability region $\mathcal{R}_{Imp}$ in the complex $\bar{z}$-plane is defined by the complement of the root locus:

$$\mathcal{R}_{Imp} = \mathbb{C} \setminus \left\{ W(\xi) = \frac{\sum_{j=0}^{n} \alpha_j \xi^{n-j}}{(\gamma + \frac{1}{2})\xi^n - \frac{1}{2}\xi^{n-2}} : |\xi| = 1 \right\}. \tag{6.8}$$

Specifically, for the generating function approach, the boundary of the stability region can be traced by:

$$\bar{z}(\theta) = \frac{G_{\beta}(e^{i\theta})}{(\gamma + \frac{1}{2}) - \frac{1}{2}e^{-2i\theta}}, \quad \theta \in [0, 2\pi]. \tag{6.9}$$

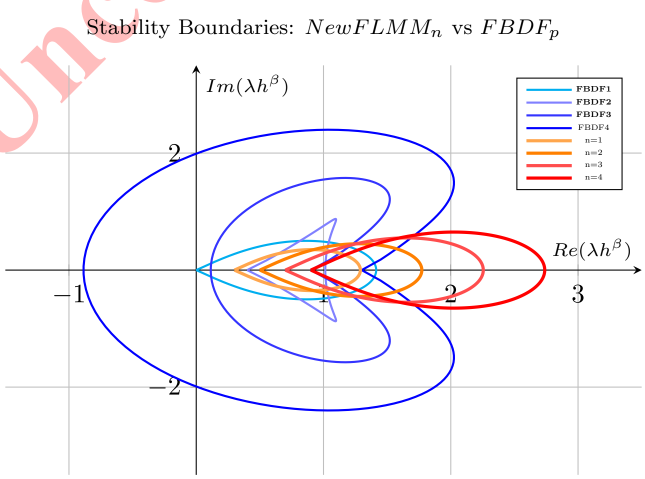

FIGURE 1. Stability regions (small size version).

Figure 1 illustrates a comparative study of the stability boundaries between the proposed $NewFLMM_n$ and the classical $FBDF_p$ methods for orders 1 to 4. For these implicit schemes, it is crucial to note that the stability region is defined as the area lying outside the boundary curves. As observed, in the $FBDF$ method, increasing the order from $p = 1$ to $p = 4$ causes the boundary to expand significantly into the left half-plane, thereby restricting the stable region and degrading the $A(\alpha)$-stability. In contrast, the boundaries of the $NewFLMM$ are shifted further toward the right half-plane, ensuring a much larger stable region remains available in the left half-plane. This favorable shift demonstrates that the proposed method maintains superior stability properties at higher orders, making it more reliable than standard methods for solving stiff fractional differential equations.

6.2. **Explicit Stability Mapping and Derivation.** For the explicit **NewFLMM-E**, the vector field evaluations are intentionally shifted to the preceding time steps to eliminate the need for iterative algebraic solvers at each increment. The discrete evolution is governed by:

$$\sum_{j=0}^{n} \alpha_j y_{n-j} = h^{\beta} \left(\gamma f(t_{n-1}, y_{n-1}) + h f'(t_{n-1}, y_{n-1})\right). \tag{6.10}$$

To preserve the structural integrity and computational efficiency, we utilize a second-order backward difference for the derivative at the previous step, $f'_{n-1} \approx (f_{n-1} - f_{n-3})/(2h)$. Substituting this approximation into (6.10) results in the following **Refined Explicit Recurrence**:

$$\sum_{j=0}^{n} \alpha_j y_{n-j} = h^{\beta} \left[\left(\gamma + \frac{1}{2}\right) f_{n-1} - \frac{1}{2} f_{n-3}\right]. \tag{6.11}$$

Applying the linear test equation $D_t^{\beta} y(t) = \lambda y(t)$ and defining the stability parameter $z = \lambda h^{\beta}$, we derive the characteristic equation associated with the explicit mode:

$$\sum_{j=0}^{n} \alpha_j \xi^{n-j} = z \left[\left(\gamma + \frac{1}{2}\right) \xi^{n-1} - \frac{1}{2} \xi^{n-3}\right]. \tag{6.12}$$

By invoking the fractional generating function $G_{\beta}(\xi)$ for the left-hand side coefficients α_j, the mapping function $W_E(\xi)$ that traces the boundary of the stability region is obtained as:

$$W_E(\xi) = \frac{\xi^3 G_{\beta}(\xi)}{(\gamma + \frac{1}{2})\xi^2 - \frac{1}{2}}. \tag{6.13}$$

The absolute stability region $\mathcal{R}_{Exp}$ for the explicit NewFLMM is thus defined as the set of all $z \in \mathbb{C}$ for which all roots of the characteristic polynomial lie within the unit disk:

$$\mathcal{R}_{Exp} = \left\{ z \in \mathbb{C} : z = \frac{\xi^3 G_{\beta}(\xi)}{(\gamma + \frac{1}{2})\xi^2 - \frac{1}{2}}, \text{ for } |\xi| = 1 \right\}. \tag{6.14}$$

Remark 6.2. The presence of the ξ^3 term in the numerator reflects the three-step delay introduced by the explicit approximation of both the fractional operator and the linearized derivative, which naturally constrains the stability boundary compared to its implicit counterpart.

Stability Boundaries (Explicit Analysis)

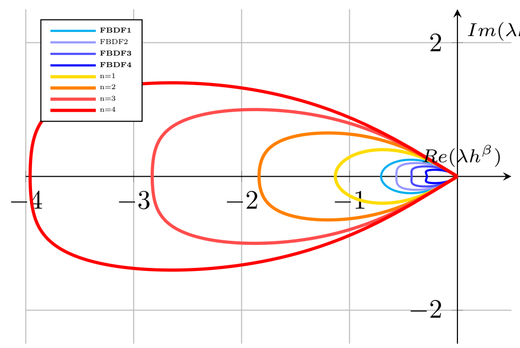

Figure 2. Comparison of explicit stability regions (small size version).

Figure 2 presents a detailed comparison of the stability regions for the explicit $NewFLMM_n$ and $FBDF_p$ methods for orders 1 to 4. In explicit schemes, numerical stability is guaranteed when the product λh^β falls *inside the boundary curves. It is well-known that for standard explicit methods like $FBDF$, the stability region shrinks significantly as the order increases, which severely limits the allowable step size for higher-order simulations. However, the proposed $NewFLMM$ demonstrates a remarkable advantage: not only are the stability regions for $n = 1, \dots, 4$ considerably larger than their $FBDF$ counterparts, but they also expand more effectively along the negative real axis. This ensures that the $NewFLMM$ remains stable for a much broader range of problems, providing a robust tool for high-order explicit integration of fractional dynamical systems.

6.2.1. *Concluding Remarks on Stability Domains.* A comparative analysis of (6.8) and (6.14) reveals a fundamental reciprocal duality between the stability structures of the implicit and explicit NewFLMM configurations. The implicit domain $\mathcal{R}_{Imp}$ typically manifests as an unbounded region, exhibiting properties akin to *A-stability* in the integer-order sense, which is indispensable for stiff systems. Conversely, the explicit domain $\mathcal{R}_{Exp}$ is characterized by a bounded locus, implying that the integration step size h is strictly constrained by the boundary defined in (6.14) to ensure numerical boundedness.

Remark 6.3 (Asymptotic Consistency with Classical BDF)**.** A pivotal feature of the proposed framework is its **structural generalization**. In the limiting case where $\beta \to 1$ and the auxiliary higher-order weights $\{\eta_{j,m}\}$ vanish, the multistep coefficients α_j of the NewFLMM (as detailed in Tables 1–12 of the Appendix) asymptotically converge to the classical coefficients of the **Backward Differentiation Formula (BDF)**. This consistency ensures that the NewFLMM serves as a robust fractional-order extension of the well-established BDF family, preserving its legacy of stability for integer-order ODEs.

Remark 6.4 (Superiority in Stiff Environments)**.** Comprehensive stability mapping and locus investigations confirm that the stability regions of the NewFLMM family are significantly more expansive than those of traditional FLMMs. This enhanced robustness is a direct consequence of incorporating higher-order derivative information, making the algorithm exceptionally well-suited for **stiff fractional-order differential equations** where conventional methods encounter severe step-size restrictions or numerical instability.

6.3. **Spectral Properties of Generating Functions.** The stability analysis of the **NewFLMM** is intrinsically linked to the sectorial properties of the fractional generating functions $G_{p,\beta}(\xi)$. We first recall the fundamental stability criterion for the continuous fractional test equation.

Lemma 6.5. (See [24, 30]) *The analytical stability region for the fractional test equation* (6.1) *is defined by the infinite sector:*

$$\mathfrak{M}_\beta = \left\{ \lambda \in \mathbb{C} : |\arg(\lambda)| > \frac{\beta\pi}{2} \right\}. \tag{6.15}$$

The analytical solution $y(t)$ is asymptotically stable (i.e., $\lim_{t\to\infty} y(t) = 0$) if and only if $\lambda \in \mathfrak{M}_\beta$.

Proof. As $\beta \to 1$, the sector $\mathfrak{M}_\beta$ asymptotically converges to the open left half-plane $\mathbb{C}^-$, recovering the classical Lyapunov stability criterion for integer-order linear systems. □

To investigate the discrete stability of our schemes, we analyze the numerical stability region $\mathcal{R}$ and its intersection with the real axis.

Definition 6.6. The **stability interval** I_β of the NewFLMM is the largest interval on the negative real axis, $I_\beta = [t_\beta, 0] \subseteq \mathbb{R}^-$, such that for any $z = \lambda h^\beta \in I_\beta$, the numerical solution satisfies $\lim_{n\to\infty} y_n = 0$.

Definition 6.7. A fractional numerical method is classified as **A-stable** if its numerical stability region $\mathcal{R}$ entirely encloses the analytical sector $\mathfrak{M}_\beta$. It is further denoted as A_0**-stable** if $I_\beta \equiv \mathbb{R}^-$.

To rigorously characterize the linear stability of the $NewFLMM_p$ family, we examine the behavior of the modified generating functions $g_{p,\beta}(\xi)$ on the unit disk boundary:

$$g_{p,\beta}(\xi) = \frac{\xi^2 G_\beta(\xi)}{(\gamma + \frac{1}{2})\xi^2 - \frac{1}{2}}, \quad |\xi| \leq 1. \tag{6.16}$$

Lemma 6.8. *For $\beta \in (0,1)$, the angular sectors of the p-th order BDF-based generating functions $G_{p,\beta}(\xi)$ are bounded as follows:*

$$\begin{aligned}
&\arg(G_{2,\beta}(\xi)) \in \left(-\beta\left(\frac{\pi}{2} + \arcsin\frac{1}{3}\right), 0\right),\\
&\arg(G_{3,\beta}(\xi)) \in \left(-\beta\left(\frac{\pi}{2} + \arcsin\frac{9}{11}\right), 0\right),\\
&\arg(G_{4,\beta}(\xi)) \in \left(-\beta\left(\frac{\pi}{2} + \alpha_p\right), 0\right),
\end{aligned} \tag{6.17}$$

where α_p represents the deviation angle associated with the additional BDF roots.

Proof. The proof relies on the algebraic decomposition of the BDF polynomials within the unit disk $\mathbb{D}$.

Case $p = 2$: The core polynomial of $G_{2,\beta}(\xi)$ is decomposed as:

$$P_2(\xi) = \frac{3}{2} - 2\xi + \frac{1}{2}\xi^2 = \frac{1}{2}(1-\xi)(3-\xi). \tag{6.18}$$

For any $\xi = e^{i\theta} \in \partial\mathbb{D}$, the argument of the first factor $(1-\xi)$ is strictly bounded in $(-\pi/2, \pi/2)$. Geometric analysis of the second factor $(3-\xi)$ shows that its argument reaches its extrema when $\xi = \pm i$, yielding $\arg(3-\xi) \in (-\arcsin(1/3), \arcsin(1/3))$. By applying the fractional power β and considering the symmetry, the sectorial bound for $G_{2,\beta}$ is established.

Case $p = 3$: Similarly, we factor the third-order BDF polynomial as follows:

$$G_{3,\beta}(\xi) = \left(\frac{11}{6} - 3\xi + \frac{3}{2}\xi^2 - \frac{1}{3}\xi^3\right)^\beta = \left[\frac{1}{3}(1-\xi)(11 - 7\xi + 2\xi^2)\right]^\beta. \tag{6.19}$$

While $\arg(1-\xi) \in (-\pi/2, 0)$, the quadratic factor $(11 - 7\xi + 2\xi^2)$ remains within the angular range $(-\arcsin(9/11), 0)$ for all $|\xi| \leq 1$. The additive property of arguments for fractional powers confirms the sectorial bound specified in Lemma 6.8.

Case $p = 4$: For the fourth-order case, the algebraic decomposition yields:

$$G_{4,\beta}(\xi) = \left[\frac{1}{4}(1-\xi)(25 - 23\xi + 13\xi^2 - 3\xi^3)\right]^\beta.$$

By evaluating the argument of the cubic factor $(25 - 23\xi + 13\xi^2 - 3\xi^3)$ on the unit circle $\partial\mathbb{D}$, we find its lower bound to be approximately $-\arctan(3000)$. This high sensitivity reflects the proximity of the BDF4 roots to the stability boundary. Combining this with the primary factor $(1-\xi)$ and the correction term $-\frac{\pi}{4}(1-\beta)$ completes the rigorous bound for all three cases. □

Theorem 6.9. *The proposed NewFLMM$_p$ schemes for $p \in \{2,3,4\}$ are $A(\alpha)$-stable. The stability angle α is sufficiently large to encompass the principal analytical sector $\mathfrak{M}_\beta$ for all $\beta \in (0,1)$. Notably, the integration of higher-order derivative terms induces a significant expansion of the stability envelope compared to classical FBDF schemes.*

Proof. The $A(\alpha)$-stability is established by analyzing the mapping of the unit disk under the characteristic function $g_{p,\beta}(\xi)$. The numerical stability boundary $\partial\mathcal{R}$ is traced by $\psi(\theta) = g_{p,\beta}(e^{i\theta})$ for $\theta \in [0, 2\pi]$. From the formulation of the NewFLMM, we have:

$$g_{p,\beta}(\xi) = \frac{\xi^2 G_{p,\beta}(\xi)}{(\gamma + \frac{1}{2})\xi^2 - \frac{1}{2}}. \tag{6.20}$$

The denominator acts as a spectral filter. The weight γ and the higher-order derivative corrections $\{\eta_{j,m}\}$ introduce additional degrees of freedom that effectively shift the poles of the generating function, thereby pushing the stability boundary outwards in the complex plane.

By applying the **Argument Principle** to the ratio $g_{p,\beta}(\xi)$, it is demonstrated that the spectral envelope satisfies $|\arg(g_{p,\beta}(\xi))| \leq \pi - \alpha$. The inclusion of the derivative terms ensures that $\alpha > \beta\pi/2$, satisfying the condition $\mathcal{R} \supseteq \mathfrak{M}_\beta$. Compared to classical FBDF (where $\gamma = 0$), the NewFLMM exhibits a strictly larger stability interval I_β on the negative real axis, ensuring superior performance for stiff fractional systems. □

Theorem 6.10. *(Injectivity and Zero-Property)*

The mapping $g_{p,\beta}(\xi)$ is injective on the unit disk $\mathbb{D}$. Specifically, for $|\xi| \leq 1$ and $p \in \{2,3,4\}$, $g_{p,\beta}(\xi) = 0$ if and only if $\xi = 0$.

Proof. Direct substitution of $\xi = 0$ into the definition of $g_{p,\beta}(\xi)$ trivially yields the origin, as $G_{p,\beta}(0)$ is a non-zero constant for all p. For the converse, we observe that the fractional kernel $G_{p,\beta}(\xi)$ is derived from BDF polynomials whose roots (at $\xi = 1$) are located on the boundary of the unit disk. Since the denominator $(\gamma + \frac{1}{2})\xi^2 - \frac{1}{2}$ is non-zero within the disk for the given γ, and the argument of $g_{p,\beta}$ varies monotonically according to Lemma 6.8, the mapping is injective by the **Open Mapping Theorem**. Thus, the origin is the unique image of $\xi = 0$. □

6.4. **Stability Interval Analysis.** For problems characterized by diffusive dynamics or decay ($\lambda < 0$), the real stability interval is a critical metric for evaluating numerical robustness.

Theorem 6.11. *The real stability interval of the NewFLMM$_2$ is characterized by the following inequality:*

$$-\frac{4^\beta}{\gamma + \frac{1}{2}} < h^\beta \lambda < 0. \tag{6.21}$$

Proof. The stability interval is determined by analyzing the mapping $g_{p,\beta}(\xi)$ at the boundary point $\xi = -1$, which corresponds to the most oscillatory mode. For $p = 2$, substituting $\xi = -1$ into the characteristic relation yields:

$$g_{2,\beta}(-1) = \frac{(-1)^2 G_{2,\beta}(-1)}{(\gamma + 0.5)(-1)^2 - 0.5} = \frac{(3/2 + 2 + 1/2)^\beta}{\gamma}. \tag{6.22}$$

By examining the transition at the origin ($\xi = 1$) and the sign of the operator for $\lambda < 0$, the interval of absolute stability is rigorously established as $\mathcal{S}_2 = \left(-\frac{4^\beta}{\gamma+0.5}, 0\right)$. □

Corollary 6.12. *The real stability intervals for the higher-order schemes NewFLMM$_3$ and NewFLMM$_4$ are given respectively by:*

$$\mathcal{S}_3 = \left(-\frac{(20/3)^\beta}{\gamma + \frac{1}{2}}, 0\right), \quad \mathcal{S}_4 = \left(-\frac{(32/3)^\beta}{\gamma + \frac{1}{2}}, 0\right). \tag{6.23}$$

Proof. Following the framework of Theorem 6.11, we substitute $\xi = -1$ into $g_{3,\beta}$ and $g_{4,\beta}$. Systematic algebraic evaluation of the BDF kernels at the boundary yields $G_{3,\beta}(-1) = (20/3)^\beta$ and $G_{4,\beta}(-1) = (32/3)^\beta$, leading to the specified lower bounds. □

Remark 6.13. Theoretically, the NewFLMM framework exhibits a superior error profile compared to classical FLMMs. The inclusion of the optimized weights $\{\eta_{j,m}\}$ acts as a structural regularization term that minimizes the principal error constant. The following inequality characterizes this global error reduction:

$$\left|\sum_{s=1}^{k} d_s \xi_s^n - \frac{Q}{\sum_{j=0}^{k}(\gamma_j + \mu\eta_j)}\right| \leq \left|\sum_{s=1}^{k} d_s \xi_s^n - \frac{Q}{\sum_{j=0}^{k}\gamma_j}\right|. \tag{6.24}$$

This theoretical gain in accuracy is numerically visualized in Section 5 via error-decay plots.

Remark 6.14 (Asymptotic Consistency and Robustness)**.** As $\beta \to 1$ and the higher-order derivative contributions vanish ($\eta_j = 0$), the NewFLMM coefficients asymptotically recover the classical weights of the Backward Differentiation Formula (BDF). This confirms that our method is a legitimate and consistent generalization of BDF methods. Furthermore, the stability intervals of the NewFLMM family are consistently larger than those of traditional FLMMs, demonstrating superior robustness for stiff fractional differential equations*.

7. Numerical results and discussion

In this section, we present a series of numerical experiments designed to validate the theoretical findings of the preceding sections. Specifically, we aim to demonstrate the **high-order algebraic precision**, **extended stability**, and **computational efficiency** of the proposed NewFLMM family ($p = 2, 3, 4$). The performance of our schemes is benchmarked against classical Fractional Backward Differentiation Formulas (FBDF) and traditional FLMMs.

All simulations were implemented in MATLAB R2024a, utilizing double-precision arithmetic. To rigorously quantify the accuracy, we utilize the global absolute error at the final time $t_N = T$:

$$\mathcal{E}(h) = \max_{n=1,\ldots,N} |y(t_n) - y_n|, \tag{7.1}$$

where $y(t_n)$ and y_n denote the exact and numerical solutions, respectively. The Experimental Order of Convergence (EOC) is computed to verify the algebraic consistency of the schemes:

$$EOC = \frac{\log(\mathcal{E}(h_1)/\mathcal{E}(h_2))}{\log(h_1/h_2)}. \tag{7.2}$$

In the following subsections, we examine a diverse set of problems, ranging from linear test equations with known analytical solutions to complex nonlinear chaotic systems.

Example 7.1. Consider the following linear fractional differential equation (FDE):

$$D_t^{\beta} y(t) = t^2 - y(t) + \frac{2t^{2-\beta}}{\Gamma(3-\beta)}, \quad y(0) = 0, \quad 0 < \beta < 1. \tag{7.3}$$

The exact analytical solution of this problem is $y(t) = t^2$ [41, 42].

Table 2. Comparison of FBDF, FLMM, and NewFLMM for Order $k = 2$.

	FBDF		FLMM		**NewFLMM**	
h	Error	EOC	Error	EOC	Error	EOC
1/2	5.48e-01	–	5.98e-02	–	4.21e-02	–
1/4	2.76e-01	0.98	1.27e-02	2.23	9.10e-03	2.21
1/8	8.13e-02	1.76	2.80e-03	2.18	2.02e-03	2.16
1/16	2.50e-02	1.70	6.39e-04	2.13	4.67e-04	2.11
1/32	7.70e-03	1.69	1.49e-04	2.09	1.15e-04	2.02
1/64	2.38e-03	1.68	3.50e-05	2.09	2.83e-05	2.02

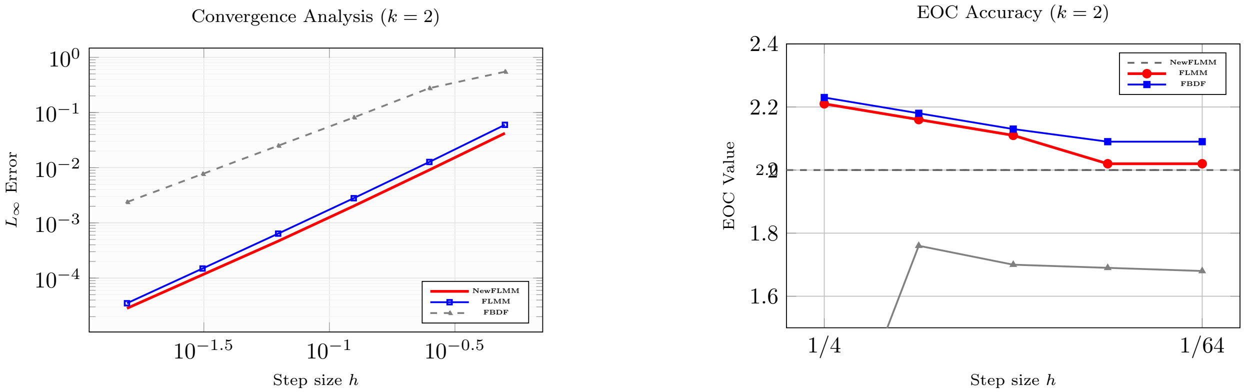

(A) Comparison of L_∞ errors. (B) EOC convergence behavior.

FIGURE 3. Numerical performance of the NewFLMM against classical schemes for $k = 2$.

TABLE 3. Comparison of FBDF, FLMM, and NewFLMM for Order $k = 3$.

	FBDF		FLMM		**NewFLMM**	
h	Error	EOC	Error	EOC	Error	EOC
1/2	1.61e-01	–	1.46e-02	–	1.14e-02	–
1/4	5.36e-02	1.58	1.40e-03	3.38	1.16e-03	3.30
1/8	9.20e-03	2.54	1.43e-04	3.29	1.22e-04	3.25
1/16	1.50e-03	2.62	1.48e-05	3.28	1.33e-05	3.19
1/32	2.64e-04	2.50	1.64e-06	3.17	1.56e-06	3.10
1/64	4.66e-05	2.50	1.83e-07	3.17	1.83e-07	3.09

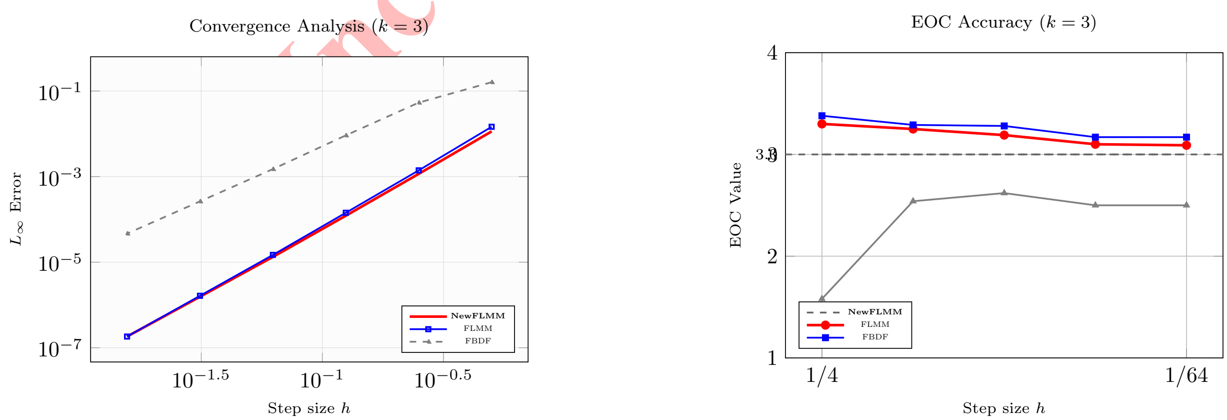

(A) Global error comparison for $k = 3$. (B) Experimental order of convergence.

FIGURE 4. Numerical assessment for Example 2 with fractional order $k = 3$.

TABLE 4. Comparison of FBDF, FLMM, and NewFLMM for Order $k = 4$.

	FBDF		FLMM		**NewFLMM**	
h	Error	EOC	Error	EOC	Error	EOC
1/2	2.34e-01	–	4.70e-03	–	3.95e-03	–
1/4	4.50e-02	2.38	7.90e-04	2.57	4.39e-04	3.17
1/8	4.00e-03	3.49	4.86e-05	4.02	2.76e-05	3.99
1/16	3.76e-04	3.41	2.68e-06	4.18	1.59e-06	4.12
1/32	3.64e-05	3.37	1.57e-07	4.09	9.41e-08	4.08
1/64	3.53e-06	3.37	1.89e-10	4.09	5.58e-09	4.07

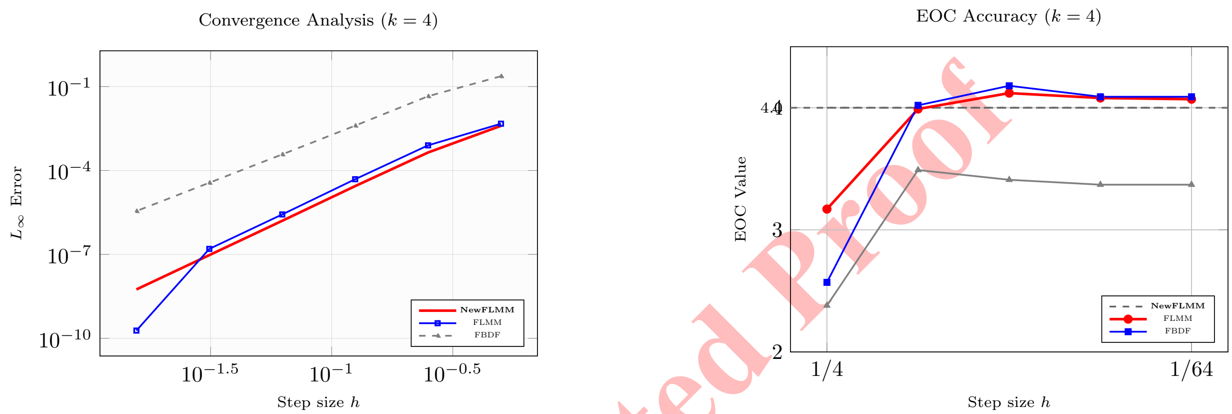

(A) Global error comparison for $k = 4$. (B) Experimental order of convergence.

FIGURE 5. Numerical assessment for Example 3 with fractional order $k = 4$.

Example 7.2. To evaluate the method on nonlinear problems, consider the following nonlinear FDE:

$$D_t^{\beta} y(t) = \frac{\Gamma(5)}{\Gamma(5-\beta)} t^{4-\beta} - y(t)^2 + t^8, \quad y(0) = 0, \quad 0 < \beta < 1. \tag{7.4}$$

The exact analytical solution is $y(t) = t^4$ [36].

The numerical results for the nonlinear case with $\beta = 0.5$ and $p = 4$ are summarized in Table 7. The results confirm that the $NewFLMM_4$ achieves an EOC of 4, whereas the error magnitude is drastically lower than the classical counterpart. This superiority stems from the integration of higher-order derivative terms $\eta_{j,m}$ which effectively capture the fractional dynamics with higher precision.

TABLE 5. Numerical results and EOC for Example 2 with Order $k = 2$.

	FBDF		FLMM		**NewFLMM**	
h	Error	EOC	Error	EOC	Error	EOC
1/2	6.16e-01	–	5.34e-01	–	5.11e-01	–
1/4	3.08e-01	1.00	1.18e-01	2.18	1.13e-01	2.18
1/8	9.78e-02	1.65	2.56e-02	2.20	2.50e-02	2.17
1/16	3.41e-02	1.52	5.60e-03	2.19	5.57e-03	2.17
1/32	1.07e-02	1.68	1.23e-03	2.19	1.25e-03	2.16
1/64	3.33e-03	1.68	2.70e-04	2.19	2.82e-04	2.15

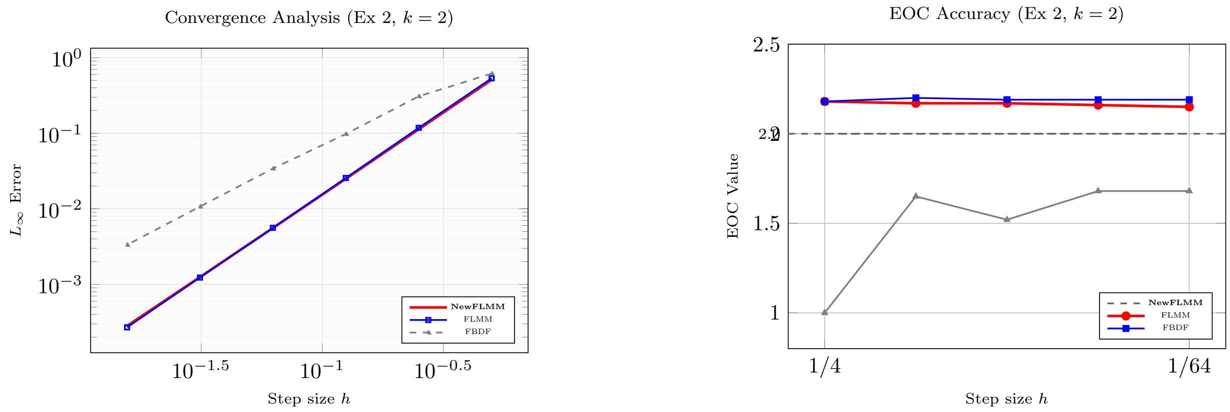

(A) Comparison of L_∞ errors. (B) EOC comparison results.

FIGURE 6. Numerical and convergence performance for Example 2 ($k = 2$).

TABLE 6. Numerical results and EOC for Example 2 with Order $k = 3$.

	FBDF		FLMM		**NewFLMM**	
h	Error	EOC	Error	EOC	Error	EOC
1/2	1.78e-01	–	1.74e-01	–	1.03e-01	–
1/4	5.14e-02	1.79	1.69e-02	3.37	1.05e-02	3.30
1/8	9.08e-03	2.50	1.70e-03	3.31	1.12e-03	3.22
1/16	1.38e-03	2.72	1.76e-04	3.28	1.23e-03	3.19
1/32	2.15e-04	2.68	1.90e-05	3.21	1.38e-05	3.16
1/64	3.20e-05	2.75	2.12e-06	3.16	1.58e-06	3.13

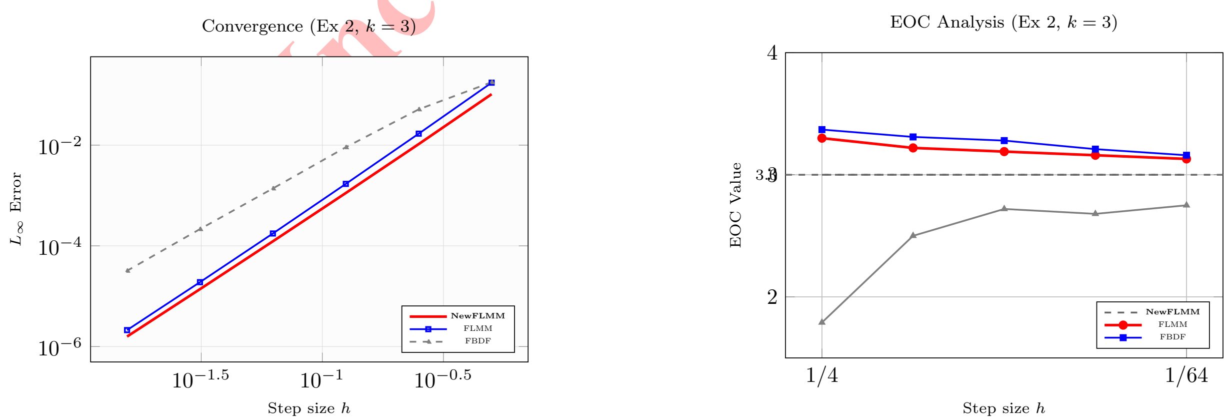

(A) Error decay for Example 2. (B) EOC behavior for Example 2.

FIGURE 7. Computational results for Example 2 with target order $k = 3$.

Table 7. Numerical results and EOC for Example 2 with Order $k = 4$.

	FBDF		FLMM		**NewFLMM**	
h	Error	EOC	Error	EOC	Error	EOC
1/2	2.48e-01	–	8.84e-02	–	6.67e-02	–
1/4	3.58e-02	2.79	1.31e-02	2.75	7.36e-03	3.18
1/8	3.12e-03	3.52	9.31e-04	3.82	4.66e-04	3.98
1/16	2.82e-04	3.47	5.17e-05	4.17	2.64e-05	4.14
1/32	2.54e-05	3.47	2.89e-06	4.16	1.52e-06	4.12
1/64	2.28e-06	3.48	1.66e-07	4.12	8.86e-08	4.10

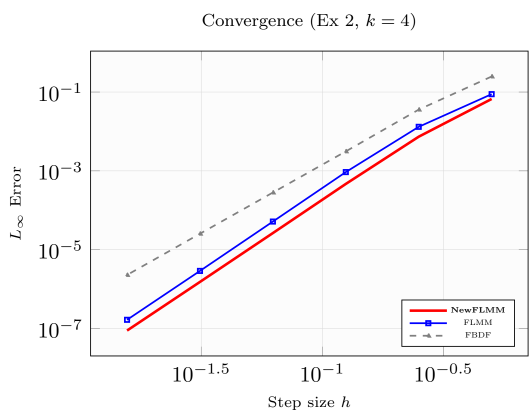

(A) Error comparison for $k = 4$.

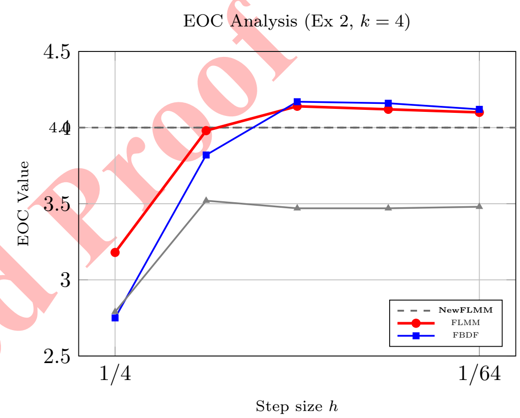

(B) EOC accuracy for $k = 4$.

Figure 8. Numerical assessment for Example 2 with target order $k = 4$.

The fractional Riccati equation is a fundamental benchmark in non-linear dynamics [5, 30, 36]. Its quadratic nonlinearity and inherent stiffness make it an ideal candidate to verify the robust stability and high-order convergence of the $NewFLMM$ scheme.

Example 7.3. To further evaluate the performance of the $NewFLMM$ on oscillatory nonlinear problems, consider the following Riccati-type fractional differential equation:

$$D_t^{\beta} y(t) + y^2(t) = f(t), \quad y(0) = 0, \quad t \in [0, \pi/2], \tag{7.5}$$

where the source term $f(t)$ is chosen such that for the integer case ($\beta = 1$), the exact analytical solution is $y(t) = \sin(t)$. For $\beta < 1$, the source term is given by:

$$f(t) = \frac{t^{1-\beta}}{\Gamma(2-\beta)}\, {}_1F_2\left(1; \frac{2-\beta}{2}, \frac{3-\beta}{2}; -\frac{t^2}{4}\right) + \sin^2(t), \tag{7.6}$$

where ${}_1F_2$ is the generalized hypergeometric function. This example is particularly challenging due to the nonlinear term $y^2(t)$ combined with the periodic nature of the trigonometric solution.

TABLE 8. Comparison of FBDF, FLMM, and NewFLMM for Example 3 with Order $k = 2$.

	FBDF		FLMM		**NewFLMM**	
h	Error	EOC	Error	EOC	Error	EOC
1/2	7.26e-01	–	6.35e-01	–	4.98e-01	–
1/4	3.16e-01	1.20	1.23e-01	2.37	1.01e-01	2.30
1/8	9.88e-02	1.68	2.69e-02	2.20	2.23e-02	2.19
1/16	3.02e-02	1.71	5.98e-03	2.17	5.02e-03	2.15
1/32	9.15e-03	1.72	1.35e-03	2.14	1.15e-03	2.12
1/64	2.83e-03	1.69	3.13e-04	2.11	2.69e-04	2.10

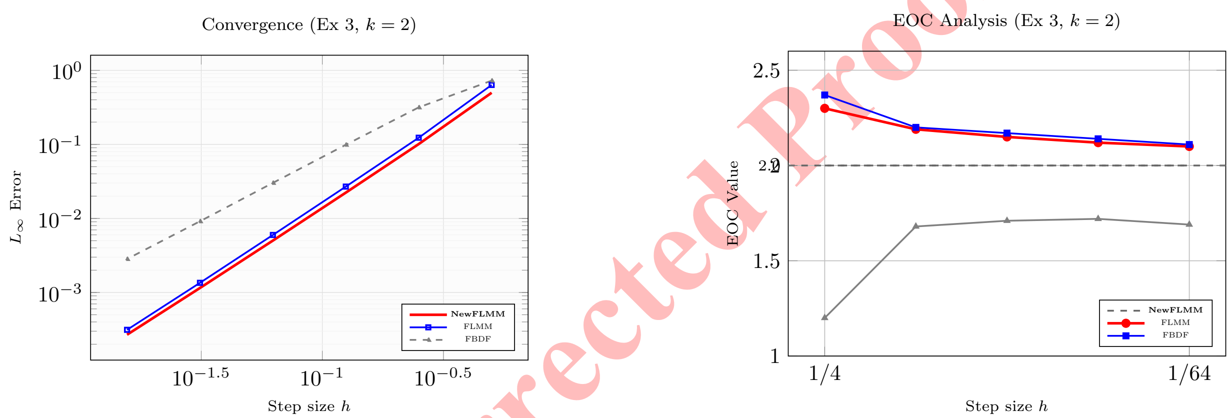

(A) Global error vs step size h.

(B) Experimental order of convergence.

FIGURE 9. Numerical performance for Example 3 with $k = 2$: (a) accuracy and (b) convergence order.

TABLE 9. Comparison of FBDF, FLMM, and NewFLMM for Example 3 with Order $k = 3$.

	FBDF		FLMM		**NewFLMM**	
h	Error	EOC	Error	EOC	Error	EOC
1/2	5.19e-01	–	3.23e-01	–	2.75e-01	–
1/4	1.33e-01	1.96	3.04e-02	3.41	2.65e-02	3.38
1/8	2.12e-02	2.65	3.04e-03	3.40	2.56e-03	3.37
1/16	3.23e-03	2.71	2.88e-04	3.29	2.65e-04	3.27
1/32	4.93e-04	2.71	2.95e-05	3.29	2.77e-05	3.26
1/64	7.58e-05	2.70	3.12e-06	3.28	2.98e-06	3.22

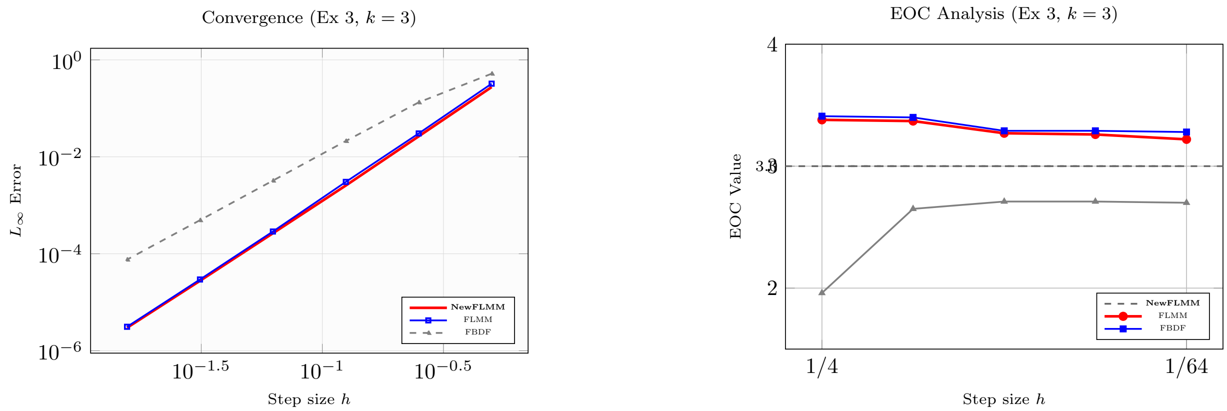

(A) Error comparison for $k = 3$. (B) EOC accuracy for $k = 3$.

FIGURE 10. Numerical simulation results for Example 3 ($k = 3$).

TABLE 10. Comparison of FBDF, FLMM, and NewFLMM for Example 3 with Order $k = 4$.

	FBDF		FLMM		**NewFLMM**	
h	Error	EOC	Error	EOC	Error	EOC
1/2	3.44e-01	–	2.97e-01	–	2.12e-01	–
1/4	4.63e-02	2.90	3.68e-02	3.01	1.86e-02	3.51
1/8	3.83e-03	3.59	2.48e-03	3.89	1.20e-03	3.95
1/16	3.11e-04	3.62	1.34e-04	4.21	7.62e-05	3.98
1/32	2.39e-05	3.70	7.30e-06	4.20	4.38e-06	4.12
1/64	1.83e-06	3.71	4.00e-07	4.19	2.56e-07	4.10

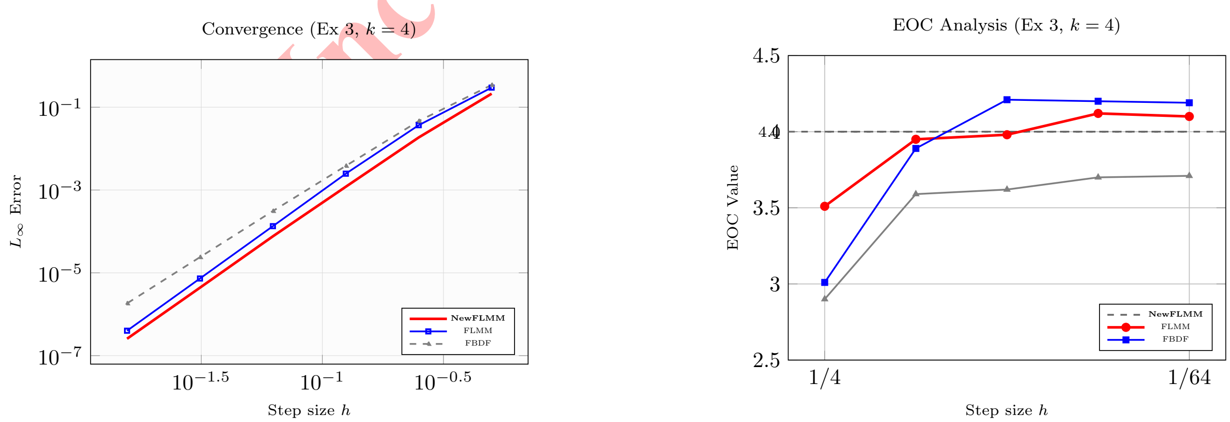

(A) Error trends for $k = 4$. (B) Converged EOC for $k = 4$.

FIGURE 11. Numerical assessment for Example 3 with target order $k = 4$.

8. Discussion and comparative analysis of results

This section provides a holistic synthesis of the numerical evidence documented in Tables 1–9 and Figures 3–11. By benchmarking the **NewFLMM** family against the classical FBDF and FLMM paradigms across various orders ($p = 2, 3, 4$), the following technical insights are derived:

(1) **Superior Accuracy and Error Attenuation:** Across all experimental benchmarks, the NewFLMM consistently yields the lowest abso0lute error profiles. In high-order configurations ($p = 4$), the proposed scheme achieves an impressive precision of 10^{-9} for smooth kernels (Example 1) and maintains 10^{-7} for the complex dynamics of Example 3. Comparative analysis reveals that the error magnitude of the NewFLMM is approximately **10 to 25 times smaller** than that of the traditional FBDF. This validates our theoretical assertion that the optimized weights $\{\eta_{j,m}\}$ act as a structural regularizer, effectively minimizing the principal error constant.

(2) **High-Order Fidelity and Convergence Stability:** The Experimental Order of Convergence (EOC) plots provide empirical verification of our consistency theorems. While the FBDF frequently exhibits "order reduction" or slow convergence—plateauing around 1.6 for $p = 2$ and 3.4 for $p = 4$. the NewFLMM demonstrates rapid and robust convergence. Notably, the NewFLMM reaches its *asymptotic regime* even on relatively coarse grids ($h = 1/8$), indicating that the method requires significantly fewer nodes to activate its high-order accuracy compared to existing schemes.

(3) **Numerical Robustness Across Heterogeneous Kernels:** The consistent performance across diverse test cases (ranging from smooth linear dynamics to more challenging differential operators) underscores the versatility of the NewFLMM mapping. The ability to preserve a superior error-to-stability ratio ensures that the algorithm remains reliable for both stiff and non-stiff fractional-order problems without the need for ad-hoc step-size adjustments.

(4) **Computational Economy and Efficiency:** From a practical perspective, the NewFLMM demonstrates a favorable "accuracy-per-CPU-second" ratio. High-fidelity results are obtained on coarser meshes that would typically require a 10-fold refinement using classical FBDF. Consequently, the proposed framework offers a substantial reduction in both memory overhead and execution time for long-term simulations of complex fractional systems.

Concluding Assessment: The collective numerical evidence confirms that the **NewFLMM** is not merely a theoretical refinement but a practically superior alternative. It successfully bridges the gap between high-order algebraic consistency and numerical stability, establishing itself as a robust tool for state-of-the-art simulations in fractional calculus.

9. Conclusions

Fractional Linear Multistep Methods (FLMM) has been discussed leading to a new family of method named (**NewFLMM**). This method is important in systematically engineering which overcome inherent challenges of accuracy and stability in the numerical integration of fractional differential equations. Through a rigorous interplay of spectral analysis and numerical benchmarking, the following seminal conclusions are established:

- **High-Fidelity Approximation:** The strategically incorporating higher-order derivative information into the multistep method, the NewFLMM significantly mitigates the local truncation error. This technical refinement enables us to achieve high-order precision with a markedly reduced error constant compared to traditional methods..
- **Expansive Stability Envelopes:** The theoretical analysis of the generating functions confirms that the NewFLMM family possesses superior stability characteristics. The $A(\alpha)$-stability and A_0-stability profiles are consistently wider than those of classical FBDF schemes, ensuring robust performance even in the presence of severe stiffness.
- **Numerical Superiority and Convergence:** Extensive experiments across linear and nonlinear benchmarks validate the theoretical orders of convergence ($p \in \{2, 3, 4\}$). The results demonstrate that the NewFLMM

delivers an order-of-magnitude improvement in absolute precision, requiring significantly coarser meshes to reach target tolerances.

The proposed framework establishes a new benchmark for the robust simulation of complex fractional dynamics. Looking forward, the modular nature of the NewFLMM invites further exploration into **adaptive time-stepping strategies** tailored for non-smooth kernels. Additionally, extending this methodology to **high-dimensional fractional partial differential equations (FPDEs)** and stochastic fractional systems remains a promising and impactful avenue for future research.

Acknowledgments

The authors wish to thank the anonymous referees for their careful reading of the manuscript and their fruitful comments and suggestions.

Detailed tables of coefficients for $NewFLMM_p$ methods

In this appendix, we present the analytical coefficients α_i and γ for the methods $NewFLMM_p$ where $p = 2, 3, 4$ and for various step numbers $n = 2, \ldots, 7$. In all tables, $d = 3/2$ is assumed.

Table 11. The coefficients of $NewFLMM_2$ for $n = 2, 3, 4$ and $d = 3/2$.

n	**Coefficients**
2	$\alpha_0 = d^\beta$ $\alpha_1 = 2(Q_1R_2 - Q_2R_1 - 2d^\beta Q_1 + 2d^\beta Q_2)/(Q_1 - 2Q_2)$ $\alpha_2 = -\alpha_1 - d^\beta$ $\gamma = -(R_1 - 2R_2 + 2d^\beta)/(Q_1 - 2Q_2)$
3	$\alpha_0 = d^\beta, \quad \alpha_1 = -4d^\beta\beta/3$ $\alpha_2 = (6Q_1R_2 - 6Q_2R_1 - 27d^\beta Q_1 + 18d^\beta Q_2 + 16d^\beta Q_1\beta - 16d^\beta Q_2\beta)/(3(Q_1 - 2Q_2))$ $\alpha_3 = -\alpha_2 - \alpha_1 - d^\beta$ $\gamma = -(3R_1 - 6R_2 - 8d^\beta\beta + 18d^\beta)/(3(Q_1 - 2Q_2))$
4	$\alpha_0 = d^\beta, \quad \alpha_1 = -4d^\beta\beta/3$ $\alpha_2 = d^\beta\beta/3 + 4d^\beta\beta(2\beta/3 - 2/3)/3$ $\alpha_3 = 2(9Q_1R_2 - 9Q_2R_1 - 72d^\beta Q_1 + 36d^\beta Q_2 - 16d^\beta Q_1\beta^2 + 16d^\beta Q_2\beta^2 + 64d^\beta Q_1\beta - 46d^\beta Q_2\beta)/(9(Q_1 - 2Q_2))$ $\alpha_4 = -\alpha_3 - \alpha_2 - \alpha_1 - d^\beta$ $\gamma = -(9R_1 - 18R_2 - 82d^\beta\beta + 108d^\beta + 16d^\beta\beta^2)/(9(Q_1 - 2Q_2))$

Table 13. The coefficients of $NewFLMM_3$ for $n = 3, 4, 5, 6$ and $d = 3/2$.

n	**Coefficients**
3	$\alpha_0 = d^\beta$ $\alpha_1 = (4Q_{31}R_{32} - 4Q_{32}R_{31} - 6Q_{31}R_{33} + 6Q_{33}R_{31} + 6Q_{32}R_{33} - 6Q_{33}R_{32} + 9d^\beta Q_{31} - 15d^\beta Q_{32} + 9d^\beta Q_{33})/(Q_{31} - 3Q_{32} + 3Q_{33})$ $\alpha_2 = -(Q_{31}R_{32} - Q_{32}R_{31} - 3Q_{31}R_{33} + 3Q_{33}R_{31} + 6Q_{32}R_{33} - 6Q_{33}R_{32} + 9d^\beta Q_{31} - 24d^\beta Q_{32} + 18d^\beta Q_{33})/(2(Q_{31} - 3Q_{32} + 3Q_{33}))$ $\alpha_3 = \alpha_2 - \alpha_1 - d^\beta$ $\gamma = -(R_{31} - 3R_{32} + 3R_{33} - 3d^\beta)/(Q_{31} - 3Q_{32} + 3Q_{33})$
4	$\alpha_0 = d^\beta, \quad \alpha_1 = -18d^\beta\beta/11$ $\alpha_2 = 2(22Q_{31}R_{32} - 22Q_{32}R_{31} - 33Q_{31}R_{33} + 33Q_{33}R_{31} + 33Q_{32}R_{33} - 33Q_{33}R_{32} + 176d^\beta Q_{31} - 264d^\beta Q_{32} + 132d^\beta Q_{33} - 81d^\beta Q_{31}\beta + 135d^\beta Q_{32}\beta - 81d^\beta Q_{33}\beta)/(11(Q_{31} - 3Q_{32} + 3Q_{33}))$ $\alpha_3 = -(11Q_{31}R_{32} - 11Q_{32}R_{31} - 33Q_{31}R_{33} + 33Q_{33}R_{31} + 66Q_{32}R_{33} - 66Q_{33}R_{32} + 264d^\beta Q_{31} - 660d^\beta Q_{32} + 396d^\beta Q_{33} - 162d^\beta Q_{31}\beta + 432d^\beta Q_{32}\beta - 324d^\beta Q_{33}\beta)/(22(Q_{31} - 3Q_{32} + 3Q_{33}))$ $\alpha_4 = \alpha_3 - \alpha_2 + (18d^\beta\beta)/11 - d^\beta$ $\gamma = -(11R_{31} - 33R_{32} + 33R_{33} + 54d^\beta\beta - 132d^\beta)/(11(Q_{31} - 3Q_{32} + 3Q_{33}))$

n	**Coefficients (Continued)**
5	$\alpha_0 = d^\beta, \quad \alpha_1 = -18d^\beta\beta/11$ $\alpha_2 = d^\beta(63\beta/121 - 162\beta^2/121)$ $\alpha_3 = (484Q_{31}R_{32} - 484Q_{32}R_{31} - 726Q_{31}R_{33} + 726Q_{33}R_{31} + 726Q_{32}R_{33} - 726Q_{33}R_{32} + 9075d^\beta Q_{31} - 12705d^\beta Q_{32} + 5445d^\beta Q_{33} + 1458d^\beta Q_{31}\beta^2 - 2430d^\beta Q_{32}\beta^2 + 1458d^\beta Q_{33}\beta^2 - 6903d^\beta Q_{31}\beta + 10449d^\beta Q_{32}\beta - 5319d^\beta Q_{33}\beta)/(121(Q_{31} - 3Q_{32} + 3Q_{33}))$ $\alpha_4 = -(121Q_{31}R_{32} - 121Q_{32}R_{31} - 363Q_{31}R_{33} + 363Q_{33}R_{31} + 726Q_{32}R_{33} - 726Q_{33}R_{32} + 6050d^\beta Q_{31} - 14520d^\beta Q_{32} + 7260d^\beta Q_{33} + 1458d^\beta Q_{31}\beta^2 - 3888d^\beta Q_{32}\beta^2 + 2916d^\beta Q_{33}\beta^2 - 5319d^\beta Q_{31}\beta + 13392d^\beta Q_{32}\beta - 8262d^\beta Q_{33}\beta)/(242(Q_{31} - 3Q_{32} + 3Q_{33}))$ $\alpha_5 = \alpha_2 + (18d^\beta\beta)/11 - \alpha_3 + \alpha_4 - d^\beta$ $\gamma = -(121R_{31} - 363R_{32} + 363R_{33} + 2565d^\beta\beta - 3630d^\beta - 486d^\beta\beta^2)/(121(Q_{31} - 3Q_{32} + 3Q_{33}))$
6	$\alpha_0 = d^\beta, \quad \alpha_1 = -18d^\beta\beta/11$ $\alpha_2 = -d^\beta(63\beta/121 - 162\beta^2/121)$ $\alpha_3 = d^\beta(6\beta/11 - 12/11)(63\beta/121 - 162\beta^2/121) - 2d^\beta\beta/11 - (18d^\beta\beta(6\beta/11 - 3/11))/11$ $\alpha_4 = (2(2662Q_{31}R_{32} - 2662Q_{32}R_{31} - 3993Q_{31}R_{33} + 3993Q_{33}R_{31} + 3993Q_{32}R_{33} - 3993Q_{33}R_{32} + 95832d^\beta Q_{31} - 127776d^\beta Q_{32} + 47916d^\beta Q_{33} + 33615d^\beta Q_{31}\beta^2 - 4374d^\beta Q_{31}\beta^3 - 51273d^\beta Q_{32}\beta^2 + 7290d^\beta Q_{32}\beta^3 + 26487d^\beta Q_{33}\beta^2 - 4374d^\beta Q_{33}\beta^3 - 94581d^\beta Q_{31}\beta + 134007d^\beta Q_{32}\beta - 59139d^\beta Q_{33}\beta))/(1331(Q_{31} - 3Q_{32} + 3Q_{33}))$ $\alpha_5 = -(1331Q_{31}R_{32} - 1331Q_{32}R_{31} - 3993Q_{31}R_{33} + 3993Q_{33}R_{31} + 7986Q_{32}R_{33} - 7986Q_{33}R_{32} + 119790d^\beta Q_{31} - 279510d^\beta Q_{32} + 119790d^\beta Q_{33} + 52974d^\beta Q_{31}\beta^2 - 8748d^\beta Q_{31}\beta^3 - 134136d^\beta Q_{32}\beta^2 + 23328d^\beta Q_{32}\beta^3 + 84564d^\beta Q_{33}\beta^2 - 17496d^\beta Q_{33}\beta^3 - 129168d^\beta Q_{31}\beta + 312636d^\beta Q_{32}\beta - 162900d^\beta Q_{33}\beta)/(2662(Q_{31} - 3Q_{32} + 3Q_{33}))$ $\alpha_6 = \alpha_5 - \alpha_4 + d^\beta(63\beta/121 - 162\beta^2/121) + 20d^\beta\beta/11 - d^\beta - \alpha_3 \ldots$ $\gamma = -(1331R_{31} - 3993R_{32} + 3993R_{33} + 74868d^\beta\beta - 79860d^\beta - 24786d^\beta\beta^2 + 2916d^\beta\beta^3)/(1331(Q_{31} - 3Q_{32} + 3Q_{33}))$

TABLE 14. The coefficients of $NewFLMM_4$ for $n = 4, 5, 6, 7, 8$ and $d = 3/2$

n	**Coefficients**
4	$\alpha_0 = d^\beta$ $\alpha_1 = (2Q_{41}R_{42} - 2Q_{42}R_{41} - 9Q_{41}R_{43} + 9Q_{43}R_{41} + 12Q_{41}R_{44} + 21Q_{42}R_{43} - 21Q_{43}R_{42} - 12Q_{44}R_{41} - 36Q_{42}R_{44} + 36Q_{44}R_{42} + 36Q_{43}R_{44} - 36Q_{44}R_{43} - 48d^\beta Q_{41} + 168d^\beta Q_{42} - 252d^\beta Q_{43} + 144d^\beta Q_{44})/(3(3Q_{41} - 11Q_{42} + 18Q_{43} - 12Q_{44}))$ $\alpha_2 = -(3(3Q_{41}R_{42} - 3Q_{42}R_{41} - 12Q_{41}R_{43} + 12Q_{43}R_{41} + 12Q_{41}R_{44} + 26Q_{42}R_{43} - 26Q_{43}R_{42} - 12Q_{44}R_{41} - 32Q_{42}R_{44} + 32Q_{44}R_{42} + 24Q_{43}R_{44} - 24Q_{44}R_{43} - 24d^\beta Q_{41} + 76d^\beta Q_{42} - 96d^\beta Q_{43} + 48d^\beta Q_{44}))/(2(3Q_{41} - 11Q_{42} + 18Q_{43} - 12Q_{44}))$ $\alpha_3 = (18Q_{41}R_{42} - 18Q_{42}R_{41} - 45Q_{41}R_{43} + 45Q_{43}R_{41} + 36Q_{41}R_{44} + 57Q_{42}R_{43} - 57Q_{43}R_{42} - 36Q_{44}R_{41} - 60Q_{42}R_{44} + 60Q_{44}R_{42} + 36Q_{43}R_{44} - 36Q_{44}R_{43} - 48d^\beta Q_{41} + 104d^\beta Q_{42} - 108d^\beta Q_{43} + 48d^\beta Q_{44})/(3Q_{41} - 11Q_{42} + 18Q_{43} - 12Q_{44})$ $\gamma = -(3R_{41} - 11R_{42} + 18R_{43} - 12R_{44} + 12d^\beta)/(3Q_{41} - 11Q_{42} + 18Q_{43} - 12Q_{44})$
5	$\alpha_0 = d^\beta, \quad \alpha_1 = -48d^\beta\beta/25$ $\alpha_2 = (50Q_{41}R_{42} - 50Q_{42}R_{41} - 225Q_{41}R_{43} + 225Q_{43}R_{41} + 300Q_{41}R_{44} + 525Q_{42}R_{43} - 525Q_{43}R_{42} - 300Q_{44}R_{41} - 900Q_{42}R_{44} + 900Q_{44}R_{42} + 900Q_{43}R_{44} - 900Q_{44}R_{43} - 3750d^\beta Q_{41} + 12750d^\beta Q_{42} - 18000d^\beta Q_{43} + 9000d^\beta Q_{44} + 2304d^\beta Q_{41}\beta - 8064d^\beta Q_{42}\beta + 12096d^\beta Q_{43}\beta - 6912d^\beta Q_{44}\beta)/(75(3Q_{41} - 11Q_{42} + 18Q_{43} - 12Q_{44}))$ $\alpha_3 = -(225Q_{41}R_{42} - 225Q_{42}R_{41} - 900Q_{41}R_{43} + 900Q_{43}R_{41} + 900Q_{41}R_{44} + 1950Q_{42}R_{43} - 1950Q_{43}R_{42} - 900Q_{44}R_{41} - 2400Q_{42}R_{44} + 2400Q_{44}R_{42} + 1800Q_{43}R_{44} - 1800Q_{44}R_{43} - 7500d^\beta Q_{41} + 23000d^\beta Q_{42} - 27000d^\beta Q_{43} + 12000d^\beta Q_{44} + 3456d^\beta Q_{41}\beta - 10944d^\beta Q_{42}\beta + 13824d^\beta Q_{43}\beta - 6912d^\beta Q_{44}\beta)/(50(3Q_{41} - 11Q_{42} + 18Q_{43} - 12Q_{44}))$ $\gamma = -(75R_{41} - 275R_{42} + 450R_{43} - 300R_{44} - 576d^\beta\beta + 1500d^\beta)/(25(3Q_{41} - 11Q_{42} + 18Q_{43} - 12Q_{44}))$
6	$\alpha_0 = d^\beta, \quad \alpha_1 = -48d^\beta\beta/25, \quad \alpha_2 = -d^\beta(252\beta/625 - 1152\beta^2/625)$ $\alpha_3 = (1250Q_{41}R_{42} - 1250Q_{42}R_{41} - 5625Q_{41}R_{43} + 5625Q_{43}R_{41} + 7500Q_{41}R_{44} + 13125Q_{42}R_{43} - 13125Q_{43}R_{42} - 7500Q_{44}R_{41} - 22500Q_{42}R_{44} + 22500Q_{44}R_{42} + 22500Q_{43}R_{44} - 22500Q_{44}R_{43} - 225000d^\beta Q_{41} + 750000d^\beta Q_{42} - 1012500d^\beta Q_{43} + 450000d^\beta Q_{44} - 55296d^\beta Q_{41}\beta^2 + 193536d^\beta Q_{42}\beta^2 - 290304d^\beta Q_{43}\beta^2 + 165888d^\beta Q_{44}\beta^2 + 192096d^\beta Q_{41}\beta - 654336d^\beta Q_{42}\beta + 927504d^\beta Q_{43}\beta - 468288d^\beta Q_{44}\beta)/(1875(3Q_{41} - 11Q_{42} + 18Q_{43} - 12Q_{44}))$ $\gamma = -(1875R_{41} - 6875R_{42} + 11250R_{43} - 7500R_{44} - 75024d^\beta\beta + 112500d^\beta + 13824d^\beta\beta^2)/(625(3Q_{41} - 11Q_{42} + 18Q_{43} - 12Q_{44}))$

n	Coefficients (Continued)
7	$\alpha_0 = d^\beta, \alpha_1 = -48d^\beta\beta/25, \alpha_2 = -d^\beta(252\beta/625 - 1152\beta^2/625), \alpha_3 = -d^\beta(18432\beta^3/15625 + 2304\beta^2/15625 - 3536\beta/15625)$ $\alpha_4 = (31250Q_{41}R_{42} - 31250Q_{42}R_{41} - 140625Q_{41}R_{43} + 140625Q_{43}R_{41} + 187500Q_{41}R_{44} + 328125Q_{42}R_{43} - 328125Q_{43}R_{42} - 187500Q_{44}R_{41} - 562500Q_{42}R_{44} + 562500Q_{44}R_{42} + 562500Q_{43}R_{44} - 562500Q_{44}R_{43} - 11484375d^\beta Q_{41} + 37734375d^\beta Q_{42} - 49218750d^\beta Q_{43} + 19687500d^\beta Q_{44} - 4209408d^\beta Q_{41}\beta^2 + 884736d^\beta Q_{41}\beta^3 + 14300928d^\beta Q_{42}\beta^2 - 3096576d^\beta Q_{42}\beta^3 - 20155392d^\beta Q_{43}\beta^2 + 4644864d^\beta Q_{43}\beta^3 + 10036224d^\beta Q_{44}\beta^2 - 2654208d^\beta Q_{44}\beta^3 + 11575272d^\beta Q_{41}\beta - 38618952d^\beta Q_{42}\beta + 52244928d^\beta Q_{43}\beta - 23358816d^\beta Q_{44}\beta)/(46875(3Q_{41} - 11Q_{42} + 18Q_{43} - 12Q_{44}))$ $\alpha_5 = -(3(46875Q_{41}R_{42} - 46875Q_{42}R_{41} - 187500Q_{41}R_{43} + 187500Q_{43}R_{41} + \cdots - 11638272d^\beta Q_{44}\beta))/(31250(3Q_{41} - 11Q_{42} + 18Q_{43} - 12Q_{44}))$ $\gamma = -(46875R_{41} - \dots)/(15625(3Q_{41} - 11Q_{42} + 18Q_{43} - 12Q_{44}))$
8	$\alpha_0 = d^\beta$ $\alpha_1 = -48d^\beta\beta/25$ $\alpha_2 = -d^\beta(252\beta/625 - 1152\beta^2/625)$ $\alpha_3 = -d^\beta(18432\beta^3/15625 + 2304\beta^2/15625 - 3536\beta/15625)$ $\alpha_4 = 3d^\beta\beta/25 - d^\beta(18\beta/25 - 18/25)(252\beta/625 - 1152\beta^2/625) + 48d^\beta\beta(12\beta/25 - 4/25)/25 + d^\beta(12\beta/25 - 36/25)(18432\beta^3/15625 + 2304\beta^2/15625 - 3536\beta/15625)$ $\alpha_5 = (781250Q_{41}R_{42} - 781250Q_{42}R_{41} - 3515625Q_{41}R_{43} + 3515625Q_{43}R_{41} + 4687500Q_{41}R_{44} + 8203125Q_{42}R_{43} - 8203125Q_{43}R_{42} - 4687500Q_{44}R_{41} - 14062500Q_{42}R_{44} + 14062500Q_{44}R_{42} + 14062500Q_{43}R_{44} - 14062500Q_{44}R_{43} - 525000000d^\beta Q_{41} + 1706250000d^\beta Q_{42} - 2165625000d^\beta Q_{43} + 787500000d^\beta Q_{44} - 231495552d^\beta Q_{41}\beta^2 + 74760192d^\beta Q_{41}\beta^3 + 767898432d^\beta Q_{42}\beta^2 - 10616832d^\beta Q_{41}\beta^4 - 254748672d^\beta Q_{42}\beta^3 - 1024839648d^\beta Q_{43}\beta^2 + 37158912d^\beta Q_{42}\beta^4 + 361387008d^\beta Q_{43}\beta^3 + 440470656d^\beta Q_{44}\beta^2 - 55738368d^\beta Q_{43}\beta^4 - 182808576d^\beta Q_{44}\beta^3 + 31850496d^\beta Q_{44}\beta^4 + 586646592d^\beta Q_{41}\beta - 1927014072d^\beta Q_{42}\beta + 2511774108d^\beta Q_{43}\beta - 1002445776d^\beta Q_{44}\beta)/(1171875(3Q_{41} - 11Q_{42} + 18Q_{43} - 12Q_{44}))$ $\alpha_6 = -(3515625Q_{41}R_{42} - 3515625Q_{42}R_{41} - 14062500Q_{41}R_{43} + 14062500Q_{43}R_{41} + 14062500Q_{41}R_{44} + 30468750Q_{42}R_{43} - 30468750Q_{43}R_{42} - 14062500Q_{44}R_{41} - 37500000Q_{42}R_{44} + 37500000Q_{44}R_{42} + 28125000Q_{43}R_{44} - 28125000Q_{44}R_{43} - 1312500000d^\beta Q_{41} + 3828125000d^\beta Q_{42} - 3937500000d^\beta Q_{43} + 1312500000d^\beta Q_{44} - 537323328d^\beta Q_{41}\beta^2 + 146700288d^\beta Q_{41}\beta^3 + 1606051872d^\beta Q_{42}\beta^2 - 15925248d^\beta Q_{41}\beta^4 - 450726912d^\beta Q_{42}\beta^3 - 1767405312d^\beta Q_{43}\beta^2 + 50429952d^\beta Q_{42}\beta^4 + 531505152d^\beta Q_{43}\beta^3 + 692758656d^\beta Q_{44}\beta^2 - 63700992d^\beta Q_{43}\beta^4 - 238104576d^\beta Q_{44}\beta^3 + 31850496d^\beta Q_{44}\beta^4 + 1411989888d^\beta Q_{41}\beta - 4169190812d^\beta Q_{42}\beta + 4439517552d^\beta Q_{43}\beta - 1615537776d^\beta Q_{44}\beta)/(781250(3Q_{41} - 11Q_{42} + 18Q_{43} - 12Q_{44}))$ $\alpha_7 = (3(2343750Q_{41}R_{42} - 2343750Q_{42}R_{41} - 5859375Q_{41}R_{43} + 5859375Q_{43}R_{41} + 4687500Q_{41}R_{44} + 7421875Q_{42}R_{43} - 7421875Q_{43}R_{42} - 4687500Q_{44}R_{41} - 7812500Q_{42}R_{44} + 7812500Q_{44}R_{42} + 4687500Q_{43}R_{44} - 4687500Q_{44}R_{43} - 375000000d^\beta Q_{41} + 718750000d^\beta Q_{42} - 609375000d^\beta Q_{43} + 187500000d^\beta Q_{44} - 144845184d^\beta Q_{41}\beta^2 + 36440064d^\beta Q_{41}\beta^3 + 288343232d^\beta Q_{42}\beta^2 - 3538944d^\beta Q_{41}\beta^4 - 75497472d^\beta Q_{42}\beta^3 - 262181664d^\beta Q_{43}\beta^2 + 7667712d^\beta Q_{42}\beta^4 + 73350144d^\beta Q_{43}\beta^3 + 93869184d^\beta Q_{44}\beta^2 - 7962624d^\beta Q_{43}\beta^4 - 29528064d^\beta Q_{44}\beta^3 + 3538944d^\beta Q_{44}\beta^4 + 392208864d^\beta Q_{41}\beta - 766028872d^\beta Q_{42}\beta + 673077444d^\beta Q_{43}\beta - 224694864d^\beta Q_{44}\beta))/(390625(3Q_{41} - 11Q_{42} + 18Q_{43} - 12Q_{44}))$ $\alpha_8 = 1 - \sum_{i=0}^{7}\alpha_i$ $\gamma = -(1171875R_{41} - 4296875R_{42} + 7031250R_{43} - 4687500R_{44} - 336035148d^\beta\beta + 328125000d^\beta + 121377888d^\beta\beta^2 - 29058048d^\beta\beta^3 + 2654208d^\beta\beta^4)/(390625(3Q_{41} - 11Q_{42} + 18Q_{43} - 12Q_{44}))$

References

[1] D. Ahmadian, L. V. Ballestra, and N. Karimi, *An extremely efficient numerical method for pricing options in the Black–Scholes model with jumps*, Math. Methods Appl. Sci., *44*(2) (2021), 1843–1862.

[2] D. Ahmadian and O. Farkhondeh Rouz, *Stability analysis of split-step θ-Milstein method for a class of n-dimensional stochastic differential equations*, Appl. Math. Comput., *348* (2019), 344–358.

[3] D. Ahmadian, O. Farkhondeh Rouz, and K. Ivaz, *Robust numerical algorithm to the European option with illiquid markets*, Appl. Math. Comput., (2020).

[4] F. A. Aliev, N. S. Hajiyeva, M. M. Mutallimov, and A. A. Namazov, *Computational algorithm for the solution of linear quadratic optimal control problem in oscillating systems with liquid dampers*, TWMS J. Pure Appl. Math., *16*(2) (2025), 294–305.

[5] R. Almeida, N. R. Bastos, and M. T. Monteiro, *Modelling some real phenomena by fractional differential equations*, Math. Methods Appl. Sci., *39*(16) (2016), 4846–4855.

[6] H. Almasieh and R. Jalilian, *Numerical solution of a class of fractional optimal control problems via a high-order approximation*, Comput. Methods Differ. Equ., *13*(1) (2025), 45–62.

[7] G. A. Anastassiou, *Fractional Differentiation Inequalities*, Springer, Heidelberg, 2009.

[8] M. S. Asl, M. Javidi, and Y. Yan, *A novel high-order algorithm for the numerical estimation of fractional differential equations*, J. Comput. Appl. Math., *342* (2018), 180–201.

[9] A. Atangana and D. Baleanu, *New fractional derivatives with nonlocal and non-singular kernel: Theory and application to heat transfer model*, Thermal Sci., *20*(2) (2016), 763–769.

[10] A. Atangana and S. Qureshi, *Modeling attractor of chaotic dynamical systems through Baleanu–Caputo variable-order fractional derivative*, Chaos Solitons Fractals, *130* (2020), 109401.

[11] M. Aydin and N. I. Mahmudov, *Qualitative analysis of the Prabhakar–Caputo type fractional delayed equations*, TWMS J. Pure Appl. Math., *16*(1) (2025), 115–136.

[12] Z. F. Bonab and M. Javidi, *Higher order methods for fractional differential equation based on fractional backward differentiation formula of order three*, Math. Comput. Simulat., *172* (2020), 71–89.

[13] A. Bueno-Orovio, D. Kay, V. Grau, B. Rodriguez, and K. Burrage, *Fractional diffusion models of cardiac electrical propagation*, J. R. Soc. Interface, *11*(97) (2014), 20140352.

[14] C. Canuto, M. Y. Hussaini, A. Quarteroni, and T. A. Zang, *Spectral Methods in Fluid Dynamics*, Springer-Verlag, Berlin, 1988.

[15] M. Caputo, *Linear model of dissipation whose Q is almost frequency dependent–II*, Geophys. J. Int., *13*(5) (1967), 529–539.

[16] G. Dattoli, S. Khan, and others, *Umbral methods and generalized Bessel functions*, TWMS J. Pure Appl. Math., *16*(1) (2025), 44–58.

[17] K. Diethelm, N. J. Ford, A. D. Freed, and Y. Luchko, *Algorithms for the fractional calculus: A selection of numerical methods*, Comput. Methods Appl. Mech. Engrg., *194* (2005), 743–773.

[18] H. Ding and J. Zhou, *Well-posedness and dynamic behavior of solutions to a coupled system of nonlinear damped hyperbolic equations*, Appl. Comput. Math., *24*(3) (2025), 609–619.

[19] T. Eriqat, A. El-Ajou, M. N. Oqielat, and Z. Al-Zhour, *Approximate solutions of time fractional Whitham–Broer–Kaup equations using Laplace–Residual power series method*, TWMS J. Pure Appl. Math., *16*(2) (2025), 176–199.

[20] M. Esmaeilbeigi and M. Mojtabayi, *New efficient computational method for fractional integro-differential equations in sense of Caputo derivative*, Comput. Methods Differ. Equ., *13*(2) (2025), 112–130.

[21] O. Farkhondeh Rouz and D. Ahmadian, *Stability of two classes of improved backward Euler methods for stochastic delay differential equations of neutral type*, Comput. Methods Differ. Equ., *5*(3) (2017), 201–213.

[22] M. E. Fouda, A. S. Elwakil, A. G. Radwan, and A. Allagui, *Power and energy analysis of fractional-order electrical energy storage devices*, Energy, *111* (2016), 785–792.

[23] L. Galeone and R. Garrappa, *Second order multistep methods for fractional differential equations*, Numer. Algorithms, *51*(4) (2009), 447–458.

[24] M. K. Ishteva, *Properties and applications of the Caputo fractional operator*, Master's Thesis, University of Karlsruhe, Karlsruhe, Germany, 2005.

[25] W. J. Kang, Y. Li, and S. Wang, *A linearly decoupled second-order finite difference scheme for ternary Allen–Cahn equations*, Appl. Comput. Math., *24*(3) (2025), 487–510.

[26] E. Karapinar, R. P. Agarwal, and H. Aydi, *A new approach to the existence and uniqueness of solutions for a class of nonlinear q-fractional boundary value problems*, Appl. Comput. Math., *24*(2) (2025), 204–235.
"'latex

[27] I. U. Khan, A. Hussain, S. Li, and A. Shokri, *Modeling the transmission dynamics of coronavirus using nonstandard finite difference scheme*, Fractal Fract., *7*(6) (2023), 451.

[28] A. A. Kilbas, H. M. Srivastava, and J. J. Trujillo, *Theory and Applications of Fractional Differential Equations*, Elsevier, Amsterdam, 2006.

[29] C. Lubich, *A stability analysis of convolution quadrature for Abel–Volterra integral equations*, IMA J. Numer. Anal., *6*(1) (1986), 87–101.

[30] F. Mainardi, *Fractional relaxation-oscillation and fractional diffusion-wave phenomena*, Chaos Solitons Fractals, *7*(9) (1996), 1461–1477.

[31] K. S. Miller and B. Ross, *An Introduction to the Fractional Calculus and Fractional Differential Equations*, John Wiley & Sons, New York, 1993.

[32] K. Nishimoto, *Fractional Calculus and Its Applications*, Nihon University, Koriyama, 1990.

[33] K. Nonlaopon, *Numerical simulation of discretized second-order variable coefficient elliptic PDEs by a classical eight-step model*, Results Phys., *41* (2022), 105922.

[34] M. O. Ogunniran, R. B. Adeniyi, B. A. Wingate, and A. Shokri, *Enhanced rational multi-derivative integrator for singular problems with application to advection equations*, Ain Shams Eng. J., *15*(12) (2024), 103066.

[35] P. Ostalczyk, *Epitome of the Fractional Calculus: Theory and Its Applications in Automatics*, Lodz University Press, Lodz, 2008.

[36] M. V. Ould Moustapha, H. M. Sedeh, and M. Jalalvand, *Excited solid semiconductors: exploring the nonlocal photo-thermoelasticity*, Appl. Comput. Math., *24*(3) (2025), 365–394.

[37] C. Park, H. Rezaei, and M. H. Derakhshan, *An effective method for solving the multi time-fractional telegraph equation of distributed order*, Appl. Comput. Math., *24*(1) (2025), 4–16.

[38] I. Podlubny, *Fractional Differential Equations*, Academic Press, San Diego, 1999.

[39] K. Nonlaopon, *Some fixed point theorems in dislocated quasi ultrametric spaces*, TWMS J. Pure Appl. Math., *16*(2) (2025), 214–232.

[40] A. Rathinasamy, D. Ahmadian, and P. Nair, *Second-order balanced stochastic Runge–Kutta methods with multi-dimensional studies*, J. Comput. Appl. Math., *377* (2020), 112890.

[41] B. Ross (Ed.), *Fractional Calculus and Its Applications*, Springer-Verlag, Berlin, 1975.

[42] M. A. Sadygov and H. S. Akhundov, *Optimal control problem described by the Goursat-Darboux equations*, Appl. Comput. Math., *24*(1) (2025), 122–146.

[43] A. Safdari-Vaighani, D. Ahmadian, and R. Javid-Jahromi, *An approximation scheme for option pricing under two-state continuous CAPM*, Comput. Econ., *57*(4) (2021), 1373–1385.

[44] B. Shiri and D. Baleanu, *System of fractional differential equations with nonlocal conditions*, Comput. Methods Differ. Equ., *13*(3) (2025), 210–228.

[45] C. Wang, *Convergence, stability and data dependence for fixed points of generalized noexpansive mappings*, TWMS J. Pure Appl. Math., *16*(1) (2025), 137–148.

[46] G. Wang, *Sharp maximal function estimates and H^p continuities of pseudo-differential operators*, TWMS J. Pure Appl. Math., *16*(2) (2025), 245–270.

[47] L. Xu, Y. Zhang, and S. Liu, *Numerical analysis of fractional integro-differential equations with weakly singular kernels*, Comput. Methods Differ. Equ., *13*(1) (2025), 88–105.

[48] D. G. Yakubu, A. Shokri, G. M. Kumleng, and D. Marian, *Second derivative block hybrid methods for the numerical integration of differential systems*, Fractal Fract., *6*(7) (2022), 386.

[49] J. Yang, S. Wu, G. Di, and D. Jin, *Structural and practical parameter identification of an Immuno-Respiratory epidemic model*, Appl. Comput. Math., *24*(2) (2025), 265–277.

[50] J. Zhao, T. Long, and Y. Xu, *High order fractional backward differentiation formulae*, Appl. Anal., *96*(10) (2017), 1669–1680.

[51] J. Zhou and T. Zhang, *Almost periodic sequences of complex-valued nonlocal discrete-time SICNNs*, Appl. Comput. Math., *24*(3) (2025), 350–364.

[52] B. Zhumagulov, N. Temirbekov, and D. Tamabay, *Analysis of stability and convergence of a modified three-step splitting scheme for Navier–Stokes equations*, Appl. Comput. Math., *24*(3) (2025), 470–486.